science for a changing world

Prepared in cooperation with the Bureau of Reclamation

Update and Recalibration of the Rio Grande Transboundary Integrated Hydrologic Model, New Mexico and Texas, United States, and Northern Chihuahua, Mexico

Scientific Investigations Report 2022–5045

U.S. Department of the Interior
U.S. Geological Survey

Cover. Photograph showing the Rio Grande near the Rio Grande at El Paso, Texas, streamgage (U.S. Geological Survey site number 08364000). Photograph by Amy E. Galanter, U.S. Geological Survey, May 2021.

Update and Recalibration of the Rio Grande Transboundary Integrated Hydrologic Model, New Mexico and Texas, United States, and Northern Chihuahua, Mexico

By Andre B. Ritchie, Amy E. Galanter, Allison K. Flickinger, Zachary M. Shephard, and Ian M. Ferguson

Prepared in cooperation with the Bureau of Reclamation

Scientific Investigations Report 2022–5045

U.S. Department of the Interior
U.S. Geological Survey

U.S. Geological Survey, Reston, Virginia: 2022

For more information on the USGS—the Federal source for science about the Earth, its natural and living resources, natural hazards, and the environment—visit https://www.usgs.gov or call 1–888–ASK–USGS.

For an overview of USGS information products, including maps, imagery, and publications, visit https://store.usgs.gov/.

Suggested citation:
Ritchie, A.B., Galanter, A.E., Flickinger, A.K., Shephard, Z.M., and Ferguson, I.M., 2022, Update and recalibration of the Rio Grande Transboundary Integrated Hydrologic Model, New Mexico and Texas, United States, and northern Chihuahua, Mexico: U.S. Geological Survey Scientific Investigations Report 2022–5045, 28 p., https://doi.org/10.3133/sir20225045.

Associated data for this publication:
Ritchie, A.B., Galanter, A.E., Flickinger, A.K., Shephard, Z.M., and Ferguson, I.M., 2022, MODFLOW One-Water Hydrologic Flow Model (MF-OWHM) used to simulate conjunctive use in the Hatch Valley and Mesilla Basin, New Mexico and Texas, United States, and northern Chihuahua, Mexico: U.S. Geological Survey data release, https://doi.org/10.5066/P99PLDXV.

ISSN 2328-0328 (online)

Contents

Figures

Table

Conversion Factors

U.S. customary units to International System of Units

Multiply	By	To obtain
	Length	
inch (in.)	2.54	centimeter (cm)
inch (in.)	25.4	millimeter (mm)
foot (ft)	0.3048	meter (m)
mile (mi)	1.609	kilometer (km)
	Area	
square mile (mi^2)	2.590	square kilometer (km^2)
	Volume	
acre-foot (acre-ft)	1,233	cubic meter (m^3)
million acre-foot (Macre-ft)	1.233	cubic kilometer (km^3)
	Flow rate	
acre-foot per year (acre-ft/yr)	1,233	cubic meter per year (m^3/yr)
acre-foot per year (acre-ft/yr)	0.001233	cubic hectometer per year (hm^3/yr)
cubic foot per day (ft^3/d)	0.02832	cubic meter per day (m^3/d)
	Hydraulic conductivity	
foot per day (ft/d)	0.3048	meter per day (m/d)

Datum

Vertical coordinate information is referenced to the North American Vertical Datum of 1988 (NAVD 88).

Horizontal coordinate information is referenced to the North American Datum of 1983 (NAD 83).

Elevation, as used in this report, refers to distance above the vertical datum.

Abbreviations

CIR	crop irrigation requirement
DEM	digital elevation model
FEI	fraction of evaporation from irrigation
FMP	Farm Process
FTR	fraction of transpiration
GHB	general head boundary
LPF	Layer-Property Flow
M&A	Montgomery & Associates
MF-OWHM	MODFLOW One-Water Hydrologic Flow Model
NWT	Newton
OFE	on-farm efficiency
PCGN	Preconditioned Conjugate Gradient Solver With Improved Nonlinear Control
R^2	coefficient of determination
RGP	Rio Grande Project
RGTIHM	Rio Grande Transboundary Integrated Hydrologic Model
RMSE	root-mean-square error
SFR2	Streamflow-Routing
UPW	Upstream Weighting
USGS	U.S. Geological Survey
WBS	water-balance subregion

Update and Recalibration of the Rio Grande Transboundary Integrated Hydrologic Model, New Mexico and Texas, United States, and Northern Chihuahua, Mexico

By Andre B. Ritchie,[1] Amy E. Galanter,[1] Allison K. Flickinger,[1] Zachary M. Shephard,[1] and Ian M. Ferguson[2]

Abstract

The Rio Grande Transboundary Integrated Hydrologic Model (RGTIHM) was developed through an interagency effort between the U.S. Geological Survey and the Bureau of Reclamation to provide a tool for analyzing the hydrologic system response to the historical evolution of water use and potential changes in water supplies and demands in the Hatch Valley (also known as Rincon Valley in the study area) and Mesilla Basin, New Mexico and Texas, United States, and northern Chihuahua, Mexico. Reclamation operates the Rio Grande Project (RGP) to store and deliver surface water for irrigation and municipal use within the study area and in the El Paso Valley south of the El Paso Narrows.

Biases in the RGTIHM's simulation of streamflow and aquifer storage depletion and the availability of new estimates of historical agricultural consumptive use in the study area initiated an update and recalibration of the RGTIHM. In addition to the new estimates of historical agricultural consumptive use, updates were made to more accurately represent the natural system and included adjustments to the initial groundwater levels; streamflow rating tables; Rio Grande, canal, and drain streambed elevations; tributary streambed elevations; surface-water inflows and diversions; RGP surface-water deliveries and canal waste; on-farm efficiency; the routing of surface-water runoff within the MODFLOW Farm Process; and general head boundaries used to simulate interbasin groundwater flow. Model settings, including the assignment of hydraulic conductivity and storage properties to model layers and the MODFLOW solver package, were adjusted to improve numerical stability, and the model was recalibrated to better simulate the natural system. The updated and recalibrated RGTIHM demonstrates a robust ability to simulate the spatially and temporally variable measurements, estimates, or reports of hydraulic head, surface-water flows, agricultural pumping, RGP surface-water deliveries and canal waste, and decadal aquifer storage changes, with improvements over the previous version of the model.

[1]U.S. Geological Survey

[2]Bureau of Reclamation

Introduction

The Rio Grande Transboundary Integrated Hydrologic Model (RGTIHM) was developed through an interagency effort between the U.S. Geological Survey (USGS) and the Bureau of Reclamation to provide a tool for analyzing the hydrologic system response to the historical evolution of water use and potential changes in water supplies and demands in the Hatch Valley (also known as Rincon Valley in the study area) and Mesilla Basin (study area), New Mexico and Texas, United States, and northern Chihuahua, Mexico (Hanson and others, 2020) (fig. 1). Reclamation operates the Rio Grande Project (RGP) to store and deliver surface water for irrigation and municipal use within the study area and in the El Paso Valley south of the El Paso Narrows (Bureau of Reclamation, 2013). Operation of the RGP includes the storage of surface water in Elephant Butte and Caballo Reservoirs, delivery of surface water through a network of irrigation canals, accounting for the application of surface water for irrigation and recharge from applied irrigation water, return flows through RGP drains and wasteways, and reuse of return flows to meet irrigation demands downstream in the RGP area. The RGTIHM provides a tool to evaluate alternative management strategies, including conjunctive management of surface water and groundwater, to support long-term planning and decision making for the RGP (Hanson and others, 2020).

Biases in the RGTIHM's simulation of streamflow and aquifer storage depletion and the availability of new estimates of historical agricultural consumptive use in the study area initiated an update and recalibration of the RGTIHM documented in Hanson and others (2020). In addition to the new estimates of historical agricultural consumptive use, updates were made to more accurately represent the natural system and included adjustments to the initial groundwater levels; streamflow rating tables; Rio Grande, canal, and drain streambed elevations; tributary streambed elevations; surface-water inflows and diversions; RGP surface-water deliveries and canal waste; on-farm efficiency (OFE); the routing of surface-water runoff within the MODFLOW Farm Process (FMP) (Schmid and Hanson, 2009); and general head boundaries (GHBs) used to simulate interbasin groundwater flow. Model settings,

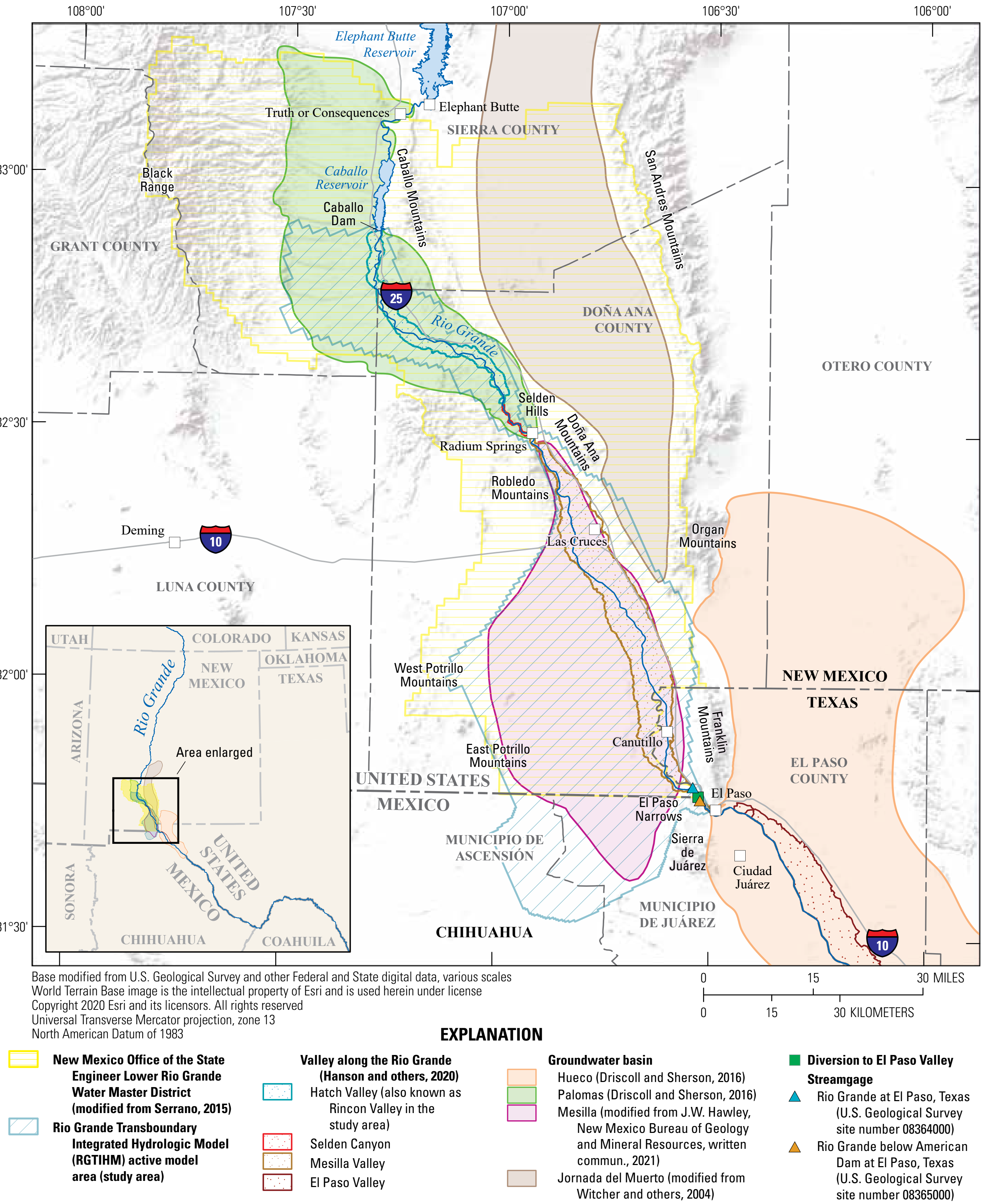

Figure 1. Study area and active model area of the Rio Grande Transboundary Integrated Hydrologic Model (RGTIHM; Hanson and others, 2020) in the Hatch Valley and Mesilla Basin, New Mexico and Texas, United States, and northern Chihuahua, Mexico.

including the assignment of hydraulic conductivity and storage properties to model layers and the MODFLOW solver package, were adjusted to improve numerical stability, and the model was recalibrated to better simulate the natural system. Recalibration of the RGTIHM was performed using PEST (Doherty, 2019), specifically BeoPEST (Schreüder, 2021), on the USGS Denali supercomputer (U.S. Geological Survey Advanced Research Computing, 2021).

Purpose and Scope

The purpose of this report is to describe the updates to the RGTIHM documented in Hanson and others (2020) and present the results and evaluate the performance of the updated and recalibrated model. Calibration results and model outputs that are discussed include (1) calibrated hydraulic conductivity and storage properties, (2) calibrated OFEs, and (3) hydrologic budgets. The performance of the updated and recalibrated RGTIHM is evaluated by comparing model simulated values against measured, estimated, or reported values for (1) hydraulic head (the elevation to which groundwater will rise in a tightly cased well; hereafter referred to as "head"), (2) surface-water flows, (3) agricultural pumping, (4) RGP surface-water deliveries and canal waste, and (5) decadal aquifer storage changes. Model performance is also evaluated in terms of mass balance errors and conceptual understanding of the hydrologic system.

Description of Study Area

The study area includes two generally northwest-southeast trending valleys that form the current floodplain of the Rio Grande: the Hatch Valley between Caballo Dam and Selden Canyon and the Mesilla Valley between Radium Springs, N. Mex., and the El Paso Narrows to the west of El Paso, Tex. (Hanson and others, 2020) (fig. 1), bounded by surrounding mesas. The Rio Grande follows the narrow valley of Selden Canyon, incised through the Selden Hills uplift, to connect the Hatch and Mesilla Valleys and exits the study area through the El Paso Narrows between the Franklin Mountains and Sierra de Juarez uplifts (Sweetkind, 2017). Inflow to the Rio Grande immediately below Caballo Dam is controlled by RGP releases from Elephant Butte and Caballo Reservoirs (Bureau of Reclamation, 2013). The study area consists of geologic structural basins, the Palomas basin[3] and the Mesilla Basin, which are bounded by uplifts: the Black Range on the northwest; the Caballo Mountains on the northeast; the San Andres, Organ, and Franklin Mountains on the east; the Sierra de Juárez and other unnamed bedrock outcrops on the south; and the East and West Potrillo Mountains on the southwest (Sweetkind, 2017).

The active model area of the RGTIHM encompasses about 1,800 square miles (mi^2) in southern New Mexico and western Texas, United States, and northern Chihuahua, Mexico (fig. 1). Land surface elevations in the study area range from 3,600 to 7,500 feet (ft) above the North American Vertical Datum of 1988 (U.S. Geological Survey, 2013a–f). The climate of the study area is arid, with hot summers and cool winters (Hanson and others, 2020). Average annual rainfall is generally less than 10 inches per year at lower elevations, with larger amounts possible at higher elevations (Hanson and others, 2020). Average annual reference evapotranspiration typically exceeds rainfall, especially at lower elevations (Hanson and others, 2020).

The hydrogeology of the study area has been discussed extensively in other reports (Sweetkind, 2017; Hanson and others, 2020), and only a summary is presented here. The principal aquifers in the study area consist of unconsolidated Pleistocene and Holocene alluvial and fluvial deposits of the Rio Grande within the current floodplain (hereafter referred to as "Quaternary alluvium") and the underlying, partly consolidated Santa Fe Group of Oligocene to Pleistocene age (Sweetkind, 2017; Hanson and others, 2020). The Santa Fe Group is subdivided into informal upper, middle, and lower hydrostratigraphic units on the basis of genesis, age, and stratigraphic position and consists of alluvial, eolian, lacustrine, and ancestral Rio Grande deposits (Hawley and Kennedy, 2004; Sweetkind, 2017). These aquifers overlie pre-Santa Fe Group rocks that include Paleogene volcanics and volcaniclastics; Cretaceous sandstones, shales, siltstones, and limestones; Paleozoic (Permian and Pennsylvanian) limestones, red beds, sandy mudstones, shales, sandstones, and gypsiferous units; and Precambrian rocks. In the Hatch Valley part of the Palomas basin, the upper Santa Fe Group unit is absent, and the primary aquifers consist of the middle Santa Fe Group unit and underlying Paleogene volcanic and volcaniclastic rocks (Hawley and Kennedy, 2004). In the northern part of the Mesilla Basin, the most productive portion of the aquifers is in ancestral Rio Grande fluvial deposits of the upper Santa Fe Group unit (Hawley and Kennedy, 2004). In the southern and western parts of the Mesilla Basin, the upper Santa Fe Group unit is in the vadose zone, and the most productive portion of the aquifers is in the middle and lower Santa Fe Group units (Hawley and Kennedy, 2004).

The study area has a complex geologic structure that developed because of tectonic events from the late Paleozoic to Mesozoic (Laramide) and subsequent Oligocene to Pleistocene deformation associated with the Rio Grande rift (Sweetkind, 2017). Rift-related extension, fault-block uplift, and basin subsidence resulted in a set of uplifted regions and structural subbasins within the members of the Santa Fe Group and pre-Santa Fe Group units that underlie the more continuous Quaternary alluvium. The Santa Fe Group was deposited in preextensional, synextensional, and postextensional settings and attains thicknesses of more than 6,000 ft with the greatest thicknesses in the Mesilla Basin being found

[3]Not an official name according to the U.S. Geologic Names Lexicon (Geolex; https://ngmdb.usgs.gov/Geolex).

adjacent to the most active fault segments (Sweetkind, 2017). The Quaternary alluvium ranges in thickness from 60 to 100 ft (Sweetkind, 2017).

Previous Model Studies

Hanson and others (2020) provided a thorough description of the history of modeling efforts in the study area. In summary, the history of model development in the study area spans several decades with incremental improvement of hydrologic simulation tools and methods for analysis of conjunctive use (Hanson and others, 2020). The RGTIHM documented in Hanson and others (2020) built on the previous modeling efforts by (1) updating the hydrogeologic framework model by using previously published and newly acquired geologic information available from wells and other investigations, (2) developing a water-balance model using the Basin Characterization Model (Flint and others, 2021) to estimate runoff and recharge from the watersheds surrounding the active model area of the RGTIHM, and (3) refining the conceptual model of the hydrologic system by using newly acquired information about natural and engineered features. Refinements to the conceptual model were incorporated in the numerical model and included (1) location and construction information for domestic, municipal, and agricultural wells, (2) surface-water and groundwater inflows and outflows, (3) the spatial distribution of land use regions, and (4) finer spatial and temporal discretization to allow simulation of smaller scale processes in the hydrologic system. In addition, Hanson and others (2020) incorporated the latest version of the MODFLOW One-Water Hydrologic Flow Model (MF-OWHM, version 2; Boyce and others, 2020), which provides the platform to allow dynamic simulation of the conjunctive use of surface water and groundwater within the study area. The RGTIHM simulates transient hydrologic conditions at 898 monthly stress periods, with 1,796 equal-interval semimonthly time steps, from March 1940 through December 2014.

Model Updates

Despite the improvements made by Hanson and others (2020) to previous modeling efforts in the study area, the RGTIHM exhibited biases in the simulation of measured surface-water flows and aquifer storage depletion estimated from changes in measured groundwater levels. At the Rio Grande at El Paso, Tex., streamgage (Rio Grande at El Paso; USGS site number 08364000; fig. 1), which was used as a key proxy for model performance relative to surface-water flows because the site is near the end of the surface-water network, near the terminus of the Mesilla Basin at the El Paso Narrows, and has a long historical measurement record spanning the full transient simulation (1940 through 2014), the RGTIHM documented in Hanson and others (2020) had a cumulative residual (simulated minus measured monthly surface-water-flow volumes) at the end of the simulation period of 4.1 million acre-feet (Macre-ft). Over the 75-year simulation period, this oversimulation bias was about 55,000 acre-feet (acre-ft) per year, which would be as much as about half of the annual inflows to the groundwater system. In addition, aquifer storage depletion simulated by Hanson and others (2020) (−0.17, −0.34, −0.09, and −0.72 Macre-ft during the 1960s, 1970s, 1990s, and 2000s, respectively) was relatively large compared to estimates derived from groundwater level changes by Rinehart and others (2016) (−0.02, −0.06, −0.10, and −0.05 Macre-ft during the 1960s, 1970s, 1990s, and 2000s, respectively). Finally, new estimates of historical agricultural consumptive use in the study area (see the "Agricultural Consumptive Use" section) became available and when incorporated in the RGTIHM documented in Hanson and others (2020) degraded the ability of the model to simulate measurements of head, surface-water flows, and agricultural pumping. All of these factors initiated the update and recalibration of the RGTIHM that are described in the following sections. In addition to the new estimates of historical agricultural consumptive use, updates were made to more accurately represent the natural system and improve numerical stability of the model.

Initial Groundwater Levels

The RGTIHM documented in Hanson and others (2020) used several published groundwater level contour maps to derive a composite estimate of hydrologic conditions before extensive groundwater development for irrigation that began in the 1950s. The resulting composite groundwater level contours were used as the initial groundwater levels in all active cells at the start of the transient simulation in March 1940. Hanson and others (2020) used scale factors on the initial groundwater levels in each of the nine model layers that were adjusted during model calibration to refine the composite estimate of initial conditions. The calibrated scale factors resulted in reductions in the initial groundwater levels and were small, ranging from a 0.095-percent reduction for layers 1 and 2 to a 0.5-percent reduction for layer 9. The RGTIHM documented in Hanson and others (2020) was sensitive to the initial groundwater levels during the early years of the transient simulation with simulated flow into (inflows) and out of (outflows) the active model area needing at least 1–2 years to stabilize. In addition, simulated surface-water flows and aquifer storage changes were sensitive throughout the simulation period to the initial groundwater levels.

The version of the RGTIHM documented in this report refined the initial groundwater levels used by Hanson and others (2020) to reduce their sensitivity and the length of time required for modeled inflows and outflows to stabilize at the beginning of the transient simulation. In some active cells, the initial groundwater levels used by Hanson and others (2020) were above the land surface elevation. Artesian groundwater conditions are not expected to be widespread in the study area, and the initial groundwater level in these cells was set to the land surface elevation. Next, a steady state spin-up approach and subsequent dynamic equilibrium spin-up approach (Anderson and others, 2015) were implemented to further refine the initial groundwater levels by simulating a longer initialization period. The steady state spin-up approach involved running the first transient stress period (March 1940) as a steady state stress period, with the initial groundwater levels set to those used by Hanson and others (2020) that were modified in this study to not be above land surface. The dynamic equilibrium spin-up approach involved running the first year (March 1940 through February 1941) of the transient simulation many times in sequence, with the simulated groundwater levels at the end (February 1941) of the previous run used as the initial groundwater levels at the beginning (March 1940) of the subsequent run. The initial groundwater levels for the first run in the dynamic equilibrium sequence were the simulated groundwater levels at the end of the steady state spin-up period.

The dynamic equilibrium spin-up was considered complete when the following three criteria were met:

1. The absolute value of the mean difference between simulated groundwater levels at each groundwater level monitoring well included in the Head-Observation package (Hill and others, 2000) at the end of successive dynamic equilibrium runs was less than 0.001 ft,

2. The absolute value of the mean difference between simulated cumulative surface-water flows at each surface-water gage location included in the HYDMOD package (Hanson and Leake, 1999) during successive dynamic equilibrium runs was less than 109 acre-ft, and

3. The absolute value of the difference between simulated cumulative net (flow into groundwater minus flow out of groundwater) aquifer storage flows in all active cells during successive dynamic equilibrium runs was less than 109 acre-ft.

The groundwater level and flow criteria for the dynamic equilibrium spin-up were set equivalent to values used by the RGTIHM documented in Hanson and others (2020) for the CLOSE_H (0.001 ft) and CLOSE_R (13,000 cubic feet per day [ft^3/d]) variables, respectively, in the Preconditioned Conjugate Gradient Solver With Improved Nonlinear Control (PCGN) package (Naff and Banta, 2008). The CLOSE_R value of 13,000 ft^3/d was converted to an annual volume, 109 acre-ft, for use as the flow criteria for the dynamic equilibrium spin-up.

The simulated groundwater levels from the end of the dynamic equilibrium spin-up were used as the initial groundwater levels for most of the recalibration of the full transient simulation (March 1940 through December 2014) described in this report. However, the model inflows and outflows had large fluctuations during the first 5–10 years of the simulation. A second steady state spin-up was implemented, with the initial groundwater levels set to the simulated groundwater levels from the end of the dynamic equilibrium spin-up, to dampen the large fluctuations in inflows and outflows. The simulated groundwater levels from the end of the second steady state spin-up were used as the initial groundwater levels for the full transient simulation described in this report. In addition, the scale factors used by Hanson and others (2020) on the initial groundwater levels were removed for the transient simulation described in this report.

Agricultural Consumptive Use

The RGTIHM documented in Hanson and others (2020) used crop irrigation requirement (CIR) values developed for the 6 agricultural canal service areas originally defined by S.S. Papadopulos and Associates, Inc. (2007) (“Arrey NM,” “Leasburg NM,” “Eastside NM,” “Eastside TX,” “Westside NM,” and “Westside TX”), to simulate agricultural consumptive use within 57 water-balance subregions (WBSs) in the FMP. A WBS is a zone within the model domain that receives surface-water deliveries or groundwater pumping from the same sources (surface-water diversion locations or wells). In the RGTIHM, these WBSs can receive either surface water and groundwater (those WBSs in the RGP) or only groundwater (those WBSs out of the RGP). The CIR values were specified monthly on the basis of data obtained from the New Mexico Office of the State Engineer (Ritchie and others, 2018; P. Barroll, New Mexico Office of the State Engineer, written commun., 2011). Hanson and others (2020) adjusted these CIR values during model calibration by climate-based, stress-coefficient scale factors. The CIR values were based on an older dataset that included estimates through 2010, with CIR values for the last 4 years of the simulation (2011 through 2014) extrapolated from years with similar annual precipitation (Hanson and others, 2020).

For this study, the CIR values were replaced with more recent and temporally complete monthly estimates of agricultural consumptive use of applied water (different terminology but equivalent in concept, as both exclude effective precipitation) spanning the full transient simulation (1940 through 2014). The estimates of agricultural consumptive use of applied water were developed by Montgomery & Associates (M&A; Schorr and Kikuchi, 2019) at the valley and RGP spatial resolution (Hatch Valley in the RGP, Hatch Valley out of the RGP, Mesilla Valley in the RGP, and Mesilla Valley out of the RGP) and spatially disaggregated within the valleys into 16 zones based on historical imagery (Hutchison, 2019). Schorr and Kikuchi (2019) estimated agricultural consumptive use from a GoldSim (GoldSim Technology Group LLC, Seattle, Washington) soil-water-balance model for fields with crops, and the estimates are provided as ancillary material in the model archive (Ritchie and others, 2022). Monthly agricultural consumptive use within the 16 zones (Hutchison, 2019) was mapped to the RGTIHM grid. First, the spatial distribution of the 16 zones was intersected with the RGTIHM grid, and the fraction of each RGTIHM grid cell corresponding to a zone or zones was calculated. Then, the agricultural consumptive use that was assigned to each grid cell was calculated as the fraction of each RGTIHM grid cell corresponding to a zone multiplied by the consumptive use of that zone and finally summed for all zones that intersected the grid cell.

The spatial extent of the 57 WBSs used in the RGTIHM documented in Hanson and others (2020) did not match the spatial extent of the 16 zones developed by LandIQ and William R. Hutchison (Hutchison, 2019). In addition, the spatial distribution of agricultural areas in and out of the RGP represented by the 57 WBSs and 16 zones did not match. Thus, the spatial extent of the 57 WBSs from Hanson and others (2020) was updated in this study so that each RGTIHM grid cell that intersected at least 1 of the 16 zones was assigned to 1 of the 57 WBSs. Also, the spatial distribution of the 57 WBSs from Hanson and others (2020) was updated in this study so that WBSs in the RGP were assigned to RGTIHM grid cells that had the largest fraction of the grid cell intersected by a zone in the RGP and WBSs out of the RGP were assigned to RGTIHM grid cells that had the largest fraction of the grid cell intersected by a zone out of the RGP.

In the FMP, the CIR is first satisfied by root uptake of groundwater if the capillary fringe above the water table is in the root zone (Hanson and others, 2020). Unlike in the RGTIHM documented in Hanson and others (2020), groundwater uptake by roots was disabled in the model described in this report because of the conceptual assumption that most of the agricultural consumption in the study area comes from applied surface water and groundwater and because the agricultural consumptive use estimates represented the consumption of applied water. The RGTIHM documented in Hanson and others (2020) used crop and irrigation style properties of the fraction of transpiration (FTR) and fraction of evaporation from irrigation (FEI) to simulate the partitioning of the CIR values between transpiration dominated during the growing season (March through October) and evaporation dominated during the nongrowing season (November through February). For this study, the agricultural consumptive use estimates were assumed to apply only to crop transpiration (FTR = 1 and FEI = 0), thereby ignoring evaporation from irrigation and groundwater. With groundwater uptake disabled and precipitation not simulated (as in the RGTIHM documented in Hanson and others, 2020), the agricultural consumptive use estimates were satisfied solely by crop transpiration from applied irrigation.

Streamflow Routing

Rating Tables

A change to the Streamflow-Routing (SFR2) package (Niswonger and Prudic, 2005) was made by refining the six-point stage-width-flow relations that were used to calculate stream depth and width. In Hanson and others (2020), stage-width-flow relations in trapezoidal channels (RGP canals and drains) were calculated from elevation survey data of the channels (Tetra Tech EM, Inc., 2004) and Manning's equation by estimating the minimum and maximum stages, width, and flow and interpolating between the minimums and maximums to estimate the other points in the rating table. In this study, the minimum and maximum stages and widths were estimated from the survey data, intermediate stages were spaced by exponentially interpolating between the minimum and maximum stages, intermediate widths were calculated from intermediate stages and channel geometry, and flows were calculated with Manning's equation using the stages and widths. The revised approach provided more stage-width-flow relations at lower flows and more evenly distributed the stage-width-flow relations across the full range of possible flows.

Rio Grande, Canal, and Drain Streambed Elevations

Hanson and others (2020) derived streambed elevations (specified in the SFR2 package as the STRTOP variable) for the Rio Grande and RGP canals and drains from light detection and ranging (International Boundary and Water Commission, 2015; U.S. Geological Survey, 2016) and digital elevation model (DEM) datasets (U.S. Geological Survey, 2013a–f). During model calibration, Hanson and others (2020) found that simulated drain flows were sensitive to the streambed elevations. To improve undersimulation of measured drain surface-water flows, Hanson and others (2020) decreased the derived streambed elevations of the Rio Grande, canals, and drains by 3 ft, which is within the assumed uncertainty associated with the streambed elevations. In this study, the streambed elevations were increased by 3 ft to the original derived elevations. The original streambed elevations were chosen to reduce the number of manual tweaks made to the RGTIHM and focus the model recalibration on other parameters sensitive to simulation of measured surface-water flows.

Tributary Streambed Elevations

Hanson and others (2020) derived tributary streambed elevations (specified in the SFR2 package as the STRTOP variable) from the DEM datasets (U.S. Geological Survey, 2013a–f). The method used to derive tributary streambed elevations along an SFR2 segment generally involved extracting the land surface elevation from the DEM at the beginning and end of each tributary segment and linearly interpolating between these endpoint elevations by using the RCHLEN variable (length of stream channel within a grid cell) to obtain streambed elevations for each reach (section of a segment that is associated with a particular grid cell). This method resulted in large differences between the top of the grid cell (defined as the land surface elevation from the DEM) and the tributary streambed elevation (maximum of about 180 ft, with an average, median, and standard deviation of 24, 17, and 24 ft below land surface, respectively). The modifications made in this study (maximum of about 150 ft, with an average, median, and standard deviation of 8.0, 4.0, and 11 ft below land surface, respectively) prevent the oversimulation of groundwater entering the tributaries that can occur in reaches with large differences between the top of the grid cell and the tributary streambed elevation.

In this study, the streambed elevation calculation process started at the most upstream reach for each tributary, where an incision of 4 ft below the land surface elevation of the model cell was used to estimate the streambed elevation of the first reach. This incision depth was used for the downstream reaches if the streambed elevation of a reach was lower than the streambed elevation of the reach directly upstream. If the calculated streambed elevation for a reach was higher than the streambed elevation of the reach directly upstream, the streambed elevation for the reach was set to 1 ft lower than the streambed elevation for the reach directly upstream to maintain a downward slope. The slopes (SLOPE variable in the SFR2 package) of the tributary reaches were recalculated using the revised STRTOP variable and RCHLEN variable.

Inflows

Specified inflow to the SFR2 package was modified from Hanson and others (2020) to represent a new conceptual understanding of the hydrologic system. El Paso Water operates the Canutillo well field near Canutillo, Tex., for production (Hanson and others, 2020). Records indicate that from 1951 through 1984 Canutillo well field pumping was discharged to the Rio Grande, conveyed via the river, and ultimately diverted and delivered to water treatment plants operated by El Paso Water (Al Blair, El Paso Valley Water Users Association, oral commun., 2021). Although records are unclear in whether all Canutillo well field pumping was discharged to the Rio Grande during this period, in this study it was assumed that all pumping was conveyed by the river through 1984, with conveyance by pipe beginning in 1985. To simulate this activity in the RGTIHM, all monthly Canutillo well field pumping from 1951 through 1984 was added as a specified inflow to the Rio Grande SFR2 segment (ISEG 375) adjacent to Canutillo.

Diversions

The RGTIHM documented in Hanson and others (2020) included monthly specified-flow diversions at nine locations along the SFR2 network, which represented the Rio Grande and RGP canals and drains. These specified-flow diversions were diversions from the Rio Grande to the Percha Lateral, Arrey Canal, Leasburg Canal, East Side Canal, and West Side Canal in New Mexico, to the El Paso Valley in Texas, and to Mexico and diversions within the canal system to WBS 1 (serving the Percha Lateral irrigation unit) and the Three Saints Lateral in New Mexico (see fig. 8*A* and *B* in Hanson and others, 2020).

For consistency with the representation of other within-canal diversions in the RGTIHM and because of a lack of data to inform the specified-flow diversions, the within-canal diversions were changed from a specified-flow diversion (SFR2 variable IPRIOR = 0) to a fractional split of the available flow in the upstream segment (SFR2 variable IPRIOR = −2). The fractional split for the diversion to WBS 1 was set to 1 so that all available flow could be diverted to WBS 1 for irrigation or returned to the Rio Grande if flow exceeded irrigation demand. The fractional split for the diversion to the Three Saints Lateral was an adjustable parameter during recalibration.

The remaining seven specified-flow diversions were compared with recent (2020) compilations of measured flow data and updated to the recent data compilations when discrepancies were found. Data for the recent compilations were obtained from Reclamation daily flow tables and monthly flow volumes provided to Reclamation by Spronk Water Engineers, Inc. (I. Ferguson, Bureau of Reclamation, written commun., 2020). Flow data for the diversion to Percha Lateral were not available prior to 1953 and from 2007 through 2009, and values were assumed to be zero during these periods. The representation of the East Side Canal specified-flow diversion was modified in this study to simulate the diversion more accurately. The RGTIHM documented in Hanson and others (2020) simulated the East Side Canal diversion by using flow data gaged on the East Side Canal downstream from the within-canal diversion to Del Rio Lateral, N. Mex. In this study, the East Side Canal diversion was simulated as the sum of the flow data gaged on the East Side Canal and the Del Rio Lateral. Del Rio Lateral flow data were not available prior to 1955 and in 1973, and values were assumed to be zero during these periods. The assumption of zero flow during periods when data were not available for the Percha and Del Rio Lateral diversions is consistent with Reclamation's monthly water distribution reports from RGP records.

Rio Grande Project Surface-Water Deliveries and Canal Waste

Monthly RGP surface-water deliveries for irrigation were used in this study as an observation dataset for recalibration and as a volumetric allotment constraint on surface-water deliveries to the WBSs simulated by the FMP in the RGTIHM. For consistency with the agricultural consumptive use inputs, RGP surface-water deliveries were estimated using data compiled by M&A (Schorr and Kikuchi, 2019). From 1940 through 1978 at the valley spatial resolution (Hatch and Mesilla Valleys), RGP surface-water deliveries compiled by Schorr and Kikuchi (2019) generally agree with delivery data compiled from Reclamation's monthly water distribution reports. After 1978, Reclamation's water distribution reports lack sufficient data for comparison with RGP surface-water deliveries compiled by Schorr and Kikuchi (2019). Schorr and Kikuchi (2019) spatially disaggregated the valleywide delivery data to the six agricultural service areas originally defined by S.S. Papadopulos and Associates, Inc. (2007). RGP surface-water deliveries compiled by Schorr and Kikuchi (2019) and from Reclamation's monthly water distribution reports are provided as ancillary material in the model archive (Ritchie and others, 2022).

Surface-water delivery observations for recalibration were organized at two spatial resolutions: (1) operational unit and (2) WBS (zones within the RGTIHM that receive surface-water deliveries or groundwater pumping from the same sources). The operational unit resolution included WBSs supplied surface water by diversions to

- Percha Lateral and Arrey Canal (Rincon operational unit; "Arrey NM" service area),
- Leasburg Canal (Leasburg operational unit; "Leasburg NM" service area), and
- East Side and West Side Canals and Del Rio Lateral (Mesilla operational unit; "Eastside NM," "Eastside TX," "Westside NM," and "Westside TX" service areas).

The WBSs associated with these operational units are summarized in table 1 in Hanson and others (2020). The surface-water delivery data disaggregated to the six agricultural service areas by Schorr and Kikuchi (2019) were further spatially disaggregated to each WBS by multiplying the delivery data for a service area by the fraction of the area of a WBS relative to the area of all WBSs associated with a service area. The surface-water delivery data disaggregated to each WBS were also used as an upper limit on the volume of surface water that could be delivered in a stress period to each WBS by the FMP. This allotment option was activated in MF-OWHM, version 2, by using the SURFACE_WATER keyword within the ALLOTMENT block of the FMP (Boyce and others, 2020).

Estimates of monthly RGP canal waste were used in this study as an observation dataset for recalibration. Canal waste represents RGP operational spills or bypass and includes El Paso Valley carriage. Observations of RGP canal waste for recalibration were estimated using data compiled from Reclamation's monthly water distribution reports from 1940 through 1978. During this period, canal waste estimates were organized at the operational unit spatial resolution: Rincon, Leasburg, and Mesilla operational units. After 1978, the organization of data in the water distribution reports changed to a coarser spatial resolution, and missing data were more common. RGP canal waste estimates compiled from Reclamation's monthly water distribution reports from 1940 through 1978 are provided as ancillary material in the model archive (Ritchie and others, 2022).

Reclamation's water distribution reports did not include surface-water deliveries or canal waste from Percha Lateral for years 1940–50 and 1954. During these years, deliveries and canal waste simulated by the RGTIHM were processed for only the Arrey Canal portion of the Rincon operational unit (WBSs 3, 5, 7, 9, and 11) for calibration to the observation datasets described above.

Farm Process

The versions of the RGTIHM documented in Hanson and others (2020) and in this report both used OFE to estimate additional water demand (applied water that is not consumed by crops) caused by inefficient irrigation. This excess irrigation was partitioned to either deep percolation to groundwater (93 percent of excess irrigation) or surface-water runoff to the SFR2 package (7 percent of excess irrigation). For consistency with the estimates of agricultural consumptive use, this study used initial estimates of annual OFE that were developed by M&A at the valley spatial resolution (Hatch and Mesilla Valleys) (Schorr and Kikuchi, 2019). Because various factors impact OFEs, the OFE values were adjusted during recalibration with a unique parameter per calendar year for the Hatch Valley and for the Mesilla Valley. The original, unadjusted values are provided as ancillary material in the model archive (Ritchie and others, 2022).

During recalibration, limits were placed on the bounds of OFEs so that values would not be less than 0.55 or greater than 0.90. These limits were determined by reviewing published estimated OFEs (Wilson, 1992; Wilson and Lucero, 1997; Wilson and others, 2003; Longworth and others, 2008). Although lesser and greater OFEs have been reported for the study area at the field scale (Ahadi and others, 2013), simulated OFE values within the updated and recalibrated RGTIHM represent average values for the Hatch and Mesilla Valleys, and OFE values less than 0.55 or greater than 0.90 are not reasonable to represent the average value for these valleys.

In the FMP, surface-water runoff can either infiltrate to groundwater as deep percolation or be aggregated by WBS and applied to the SFR2 package as runoff. In Hanson and others (2020) and this study, all surface-water runoff infiltrated to groundwater for those WBSs out of the RGP area. In Hanson and others (2020), surface-water runoff for the WBSs in the RGP area was applied to all nondiversion SFR2 reaches in a WBS, prorated by the length of each reach in a WBS. As a result, a substantial portion of the surface-water runoff was routed into canals, which is unrealistic. In the RGP area, surface-water runoff of applied irrigation is generally routed to drains or directly back to the Rio Grande because canals are at higher elevations than the agricultural fields to allow gravity flow from canal to field and because surface-water runoff of applied irrigation often carries salts and sediments that are not desirable for agriculture. In this study, surface-water runoff for the WBSs in the RGP area was applied only to drain or Rio Grande SFR2 reaches in a WBS.

As discussed in the "Agricultural Consumptive Use" section, the RGTIHM documented in Hanson and others (2020) simulated agricultural consumptive use within 57 WBSs in the FMP. In addition, Hanson and others (2020) simulated transpiration from native vegetation, urban landscapes, and golf courses within 12 additional WBSs. In this study, transpiration from native vegetation was assumed to be negligible compared with crop transpiration and was ignored. This assumption is reasonable because most of the native vegetation region simulated by Hanson and others (2020) was outside the Rio Grande Valley, where groundwater levels are typically below the root zone of native vegetation (Wilson and others, 1981), and Hanson and others (2020) and this study do not simulate precipitation, which could be another likely source for transpiration by native vegetation. In this study, transpiration from urban landscapes and golf courses was not explicitly simulated, but the extent of these WBSs as simulated by Hanson and others (2020) was generally incorporated in the extent of the 57 WBSs used in this study to simulate agricultural consumptive use.

General Head Boundaries

GHBs were used in the RGTIHM to simulate interbasin groundwater flow at the Rincon Arroyo in the Hatch Valley, through the area locally referred to as “Fillmore Pass” (Hawley and Lozinsky, 1992) in the eastern part of the Mesilla Basin, through the El Paso Narrows, and through the southern boundary of the model in Mexico (see fig. 17 in Hanson and others [2020]). In this study, modifications were made to the Bhead variable (the head on the boundary) in the General-Head Boundary (GHB) package (Harbaugh and others, 2000) to align more closely with the modified initial groundwater levels (described in the “Initial Groundwater Levels” section). Groundwater flux at the GHBs is proportional to the difference between head on the boundary and within the active model cells adjacent to the boundary. Modifications to the boundary head were made to prevent an excessive flux of groundwater at the GHBs during early periods of the transient simulation. As in Hanson and others (2020), these boundary heads were held constant in time during the transient simulation because of a lack of historical measurements of head along the GHBs. The annual net flow (inflow minus outflow) associated with the GHBs was less than 1 percent of the total annual net flow for the entire groundwater system, and thus the GHBs have a negligible impact on the simulation.

Layering

The RGTIHM uses nine layers, with each layer corresponding to a unique hydrostratigraphic unit based on the hydrogeologic framework model described in Sweetkind (2017) and Sweetkind and others (2017). Hanson and others (2020) used phantom cells within the RGTIHM’s structured finite-difference grid when individual hydrostratigraphic layers were not physically present in the subsurface. In this approach, phantom cell horizontal hydraulic conductivities and storage properties were set to a small number, and phantom cell vertical hydraulic conductivities were set to a number large enough to allow vertical flow between the vertically adjacent layers (as described in Faunt [2009]). In this study, an alternative approach was taken by assigning phantom cell hydraulic conductivity and storage properties equal to the properties of the next (below) adjacent layer that was physically present in the subsurface (as described in Macfarlane [1995] and Anderson and others [2015]). This approach removed the extreme phantom cell hydraulic conductivity and storage properties from the model while adding the phantom cell vertical thickness (5 ft) to some hydrostratigraphic layers. This approach was chosen for this study because of the possibility of improved numerical stability created by removing the large horizontal and vertical fluctuations in hydraulic conductivity and storage properties created by the phantom cells and because the phantom cell vertical thickness added to the physically present hydrostratigraphic layers was assumed to be within the uncertainty of the hydrostratigraphic layer thicknesses from the hydrogeologic framework model.

Solver

As mentioned in the “Initial Groundwater Levels” section, the RGTIHM documented in Hanson and others (2020) used the PCGN solver package. In this study, the Newton (NWT) solver package was used to solve the finite difference equations in each time step of the monthly stress periods. The NWT solver package can only be used with the Upstream Weighting (UPW) package (Niswonger and others, 2011), which replaced the Layer-Property Flow (LPF) package (Harbaugh and others, 2000) used in Hanson and others (2020). The UPW and LPF packages have identical input except for the inclusion of the IPHDRY variable (set equal to zero in this study) in the UPW package. All layers in the RGTIHM are simulated as confined; thus, the UPW and LPF packages behave identically. The NWT solver package was chosen for this study because it resulted in lower model mass balance errors than did the PCGN solver package at similar solver convergence criteria (HEADTOL and FLUXTOL variables in the NWT solver package and CLOSE_H and CLOSE_R variables in the PCGN solver package).

Decadal Aquifer Storage Changes

Estimates of aquifer storage changes for the “El Paso-Las Cruces basin” developed by Rinehart and others (2016) were used in this study as an observation dataset for recalibration. Rinehart and others (2016) used groundwater levels measured from the 1950s through the 2010s along with estimates of specific yield to calculate aquifer storage changes in the alluvial aquifers of the Rio Grande rift basins, with aquifer storage change summarized by surface watersheds. The groundwater level measurements were obtained from well networks with limited spatial coverage within each watershed, and thus the calculated aquifer storage declines are likely underestimates (Rinehart and others, 2016). The cumulative aquifer storage changes presented in Rinehart and others (2016) were incorporated as decadal storage change observations for recalibration of the RGTIHM. For example, the table in Rinehart and others (2016) shows cumulative aquifer storage change from the 1950s of −0.02 Macre-ft by the 1960s and −0.08 Macre-ft by the 1970s, where negative values indicate a decrease in aquifer storage. Thus, for this study, simulated decadal aquifer storage changes for the entire RGTIHM domain from the beginning of the 1960s through the end of the 1960s (1960s) and from the beginning of the 1970s through the end of the 1970s (1970s) were calibrated to the Rinehart and others (2016) estimates of −0.02 Macre-ft and −0.06 Macre-ft, respectively. Decadal aquifer storage change estimates for the 1980s, 1990s, and 2000s were incorporated as observation datasets in a similar manner. Aquifer storage change estimates for the 2010s were not incorporated as an observation dataset for calibration because the RGTIHM only simulates through 2014, and it was unclear how much of the 2010s the Rinehart and others (2016) estimate included.

Model Recalibration

Recalibration of the RGTIHM was performed using PEST, specifically BeoPEST (Schreüder, 2021). BeoPEST was run using the USGS Denali supercomputer (U.S. Geological Survey Advanced Research Computing, 2021). The suite of parameters that was adjusted during recalibration was mostly unchanged from Hanson and others (2020), but new parameters were added to adjust the annual OFEs provided by Schorr and Kikuchi (2019), and vertical anisotropy was used in the UPW package rather than vertical hydraulic conductivity. Parameters that were adjusted during recalibration included horizontal hydraulic conductivity, vertical anisotropy, and specific storage of model layers; hydraulic conductance within the GHB package; hydraulic characteristic within the Horizontal Flow Barrier package (Hsieh and Freckleton, 1993); streambed hydraulic conductivity within the SFR2 package; fractional splits of the flow in the segment upstream from diversion points along the SFR2 network where water is diverted within canal from main canals to smaller canals; and annual OFEs for the Hatch and Mesilla Valleys.

Adjustments to parameter values during recalibration were based on the ability of model simulated values to reproduce measurements, estimations, or reports of head, surface-water flows, agricultural pumping, RGP surface-water deliveries and canal waste, and decadal aquifer storage changes. The RGP surface-water deliveries and canal waste and the aquifer storage changes described in the “Model Updates” section were added as new observation datasets, and more surface-water-flow measurements were included in the recalibration; otherwise, observations for recalibration were unchanged from Hanson and others (2020). Observation weights within PEST were applied to give relatively more importance to surface-water flows and RGP surface-water deliveries and canal waste compared to the other observations to focus the recalibration on reducing the RGTIHM’s biases in the simulation of measured surface-water flows. In addition, surface-water observations were given more importance in PEST to offset the effect of the large number of head observations (59,130) relative to the number of surface-water-flow (24,480) and RGP surface-water delivery (34,124) and canal waste (1,398) observations.

Calibration Results and Model Outputs

Selected calibration results and model outputs are discussed in this section. Calibrated hydraulic conductivity and storage properties and OFEs are summarized because these parameters affect groundwater flow, groundwater/surface-water interaction, delivery of surface water to WBSs, recharge of applied irrigation water, and return flows to RGP drains and wasteways. The hydrologic budget summarizes the magnitude and components of annual simulated flows into and out of the groundwater system.

Hydraulic Conductivity and Storage Properties

The range of hydraulic conductivity and specific storage values by layer and hydrostratigraphic unit that resulted from the recalibration of the updated RGTIHM is summarized in table 1. In the RGTIHM, layers 1 and 2 represent the Quaternary alluvium, layers 3 and 4 represent the upper Santa Fe Group, layers 5 and 6 represent the middle Santa Fe Group, layers 7 and 8 represent the lower Santa Fe Group, and layer 9 represents the pre-Santa Fe Group units. Overall, hydraulic conductivity and specific storage values were within the range of literature values reported for hydrogeologic units of similar lithology. In the RGTIHM, each layer is subdivided into zones that represent different sedimentary facies within the hydrostratigraphic units. During recalibration, horizontal hydraulic conductivity values for each sedimentary facies zone could vary within the ranges presented in Hawley and Kennedy (2004, tables 3-2 and 3-3), thereby providing an additional constraint on calibration. The horizontal hydraulic conductivity values show a decreasing trend with increasing depth, especially in the Santa Fe Group as finer grained lithofacies become more common in the middle and lower Santa Fe Group (Sweetkind, 2017).

All layers in the RGTIHM are simulated as confined in MF-OWHM and thus require the specification of specific storage. In model layers that may behave in an unconfined manner, assumed to be the uppermost active layer in each model row and column location, specific storage was estimated as specific yield divided by the cell thickness plus the compressibility of water (Hanson and others, 2020). The maximum specific storage values presented in table 1 are assigned to these “unconfined” grid cells to represent the uptake and release of water to and from aquifer storage, respectively, due to gravity-driven draining or filling of the saturated thickness of the aquifer.

Table 1. Range of recalibrated horizontal and vertical hydraulic conductivities and specific storage by layer and hydrostratigraphic unit for the updated Rio Grande Transboundary Integrated Hydrologic Model (RGTIHM) documented in this report.

Model layers	Hydrostratigraphic unit	Horizontal hydraulic conductivity (feet per day)		Vertical hydraulic conductivity (feet per day)		Specific storage (foot^{-1})	
		Minimum	Maximum	Minimum	Maximum	Minimum	Maximum
1 and 2	Quaternary alluvium	0.14	100	0.00014	92	0.0000068	0.0060
3 and 4	Upper Santa Fe Group[1]	0.010	100	0.00074	100	0.0000014	0.13
5 and 6	Middle Santa Fe Group[1]	0.016	100	0.000034	30	0.00000047	0.16
7 and 8	Lower Santa Fe Group[1]	0.024	2.2	0.000040	0.92	0.0000010	0.0061
9	Pre-Santa Fe Group[1]	0.0042	10	0.00033	0.34	0.00000073	0.00060

[1]Informal names.

On-Farm Efficiencies

OFEs are used in the RGTIHM to account for irrigation losses. The OFE reflects the distribution and application of water on a field (Jensen, 1967; Magnuson and others, 2019). Field conditions that can affect OFEs include crop root depth at the time of irrigation, soil type and soil moisture, irrigation system (type, infrastructure, water quality), field attributes (slope, length, width, land surface preparation), and farm management (frequency and amount of irrigation application) (Magnuson and others, 2019). In MF-OWHM, the irrigation demand is calculated by dividing the consumptive irrigation requirement by the OFE (Boyce and others, 2020). Because the RGTIHM does not simulate precipitation, simulated OFEs do not account for effective precipitation and therefore are likely larger than OFE values from other studies in which the OFE is calculated by subtracting effective precipitation from the evapotranspiration demand (Ahadi and others, 2013; Magnuson and others, 2019; Schorr and Kikuchi, 2019).

OFEs simulated by the updated and recalibrated RGTIHM vary annually, so a 5-year moving average (average of the previous 2 years, the current year, and the following 2 years) was calculated for the Hatch Valley and the Mesilla Valley to provide perspective on the long-term trends (fig. 2*A*). The 5-year moving averages for simulated OFEs in the Hatch and Mesilla Valleys show long-term increases, with values below 0.65 in the beginning of the simulation and higher values, near 0.80, towards the end of the simulation. Figure 2*A* also shows wet and dry climate periods that were calculated by calendar year and are based on the cumulative departure from the average of annual surface-water releases from Caballo Reservoir (calculated in Hanson and others, 2020).

A correlation between releases from Caballo Reservoir (fig. 2*B*) and OFEs in the Hatch and Mesilla Valleys (fig. 2*A*) was expected (increasing OFEs during dry climate periods with lower surface-water releases from Caballo Reservoir and decreasing or relatively unchanged OFEs during wet climate periods with higher surface-water releases from Caballo Reservoir). This expected correlation is not always apparent in the annual OFEs or the 5-year moving averages. While some dry climate periods corresponded with increasing 5-year moving averages of OFEs and some wet climate periods corresponded to decreasing or relatively unchanged 5-year moving averages of OFEs, annual OFEs were quite variable (fig. 2*A*). Although average annual OFEs for each valley are simplifications of the spatial and temporal complexities of OFEs within the study area, the long-term trends observed in the simulated OFEs show a reasonable representation of irrigation practices from 1940 through 2014.

Hydrologic Budget

The annual net (inflow minus outflow) groundwater flow budget simulated by the updated and recalibrated RGTIHM is presented in figure 3 as a stacked bar chart with budget components contributing to a net outflow from the groundwater system plotted below zero net flow and budget components contributing to a net inflow to the groundwater system plotted above zero net flow. Change in aquifer storage serves as either a source (flow from aquifer storage to groundwater; that is, depletion of aquifer storage) or sink (flow to aquifer storage from groundwater; that is, accumulation of aquifer storage) of groundwater flow. Thus, in figure 3, depletion of aquifer storage is represented as a positive net budget component, and accumulation of aquifer storage is represented as a negative net budget component.

For the 1940s, the RGTIHM generally simulates aquifer storage accumulation (fig. 3). Most of this storage accumulation happens in layer 1 of the model, which represents the unconfined Quaternary alluvium within the current floodplain of the Rio Grande and is primarily sourced by deep percolation to groundwater from the WBSs (“Farm Process farm net recharge” on fig. 3). Agricultural well pumping increased during the 1940s as more wells were installed to supply water to meet WBS demand (Hanson and others, 2020). The Rio Grande and its tributaries and RGP canals and drains (“Rio Grande, tributaries, and Rio Grande Project canals and drains” on fig. 3) are generally gaining flow from groundwater through the 1940s.

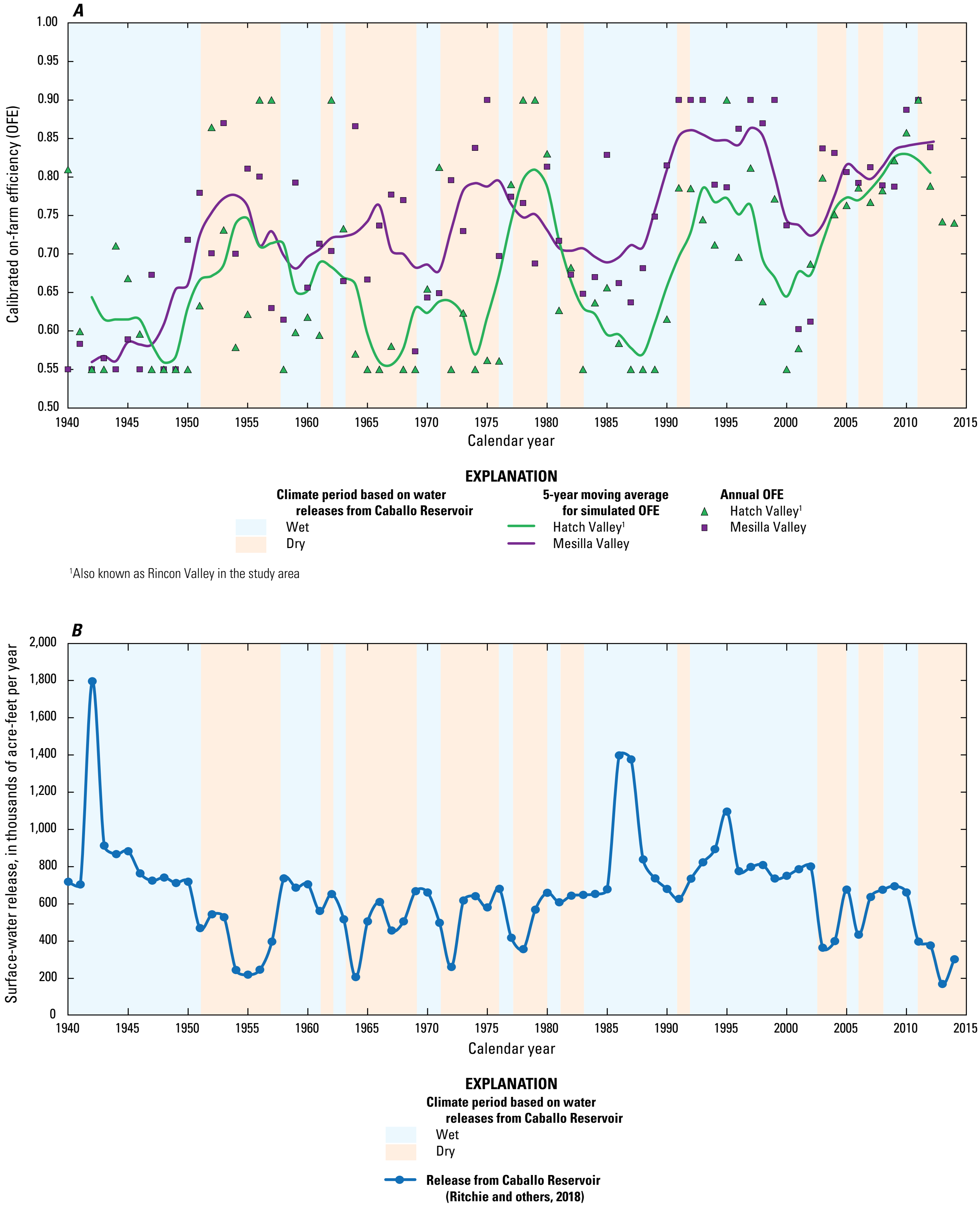

Figure 2. *A*, Calibrated on-farm efficiencies for the Hatch Valley and Mesilla Valley and respective 5-year moving averages, 1940 through 2014, and *B*, monthly surface-water releases from Caballo Reservoir aggregated by calendar year, 1940 through 2014, for the Rio Grande Transboundary Integrated Hydrologic Model, New Mexico and Texas, United States, and northern Chihuahua, Mexico. Climate periods are based on cumulative departure from average of annual surface-water releases from Caballo Reservoir.

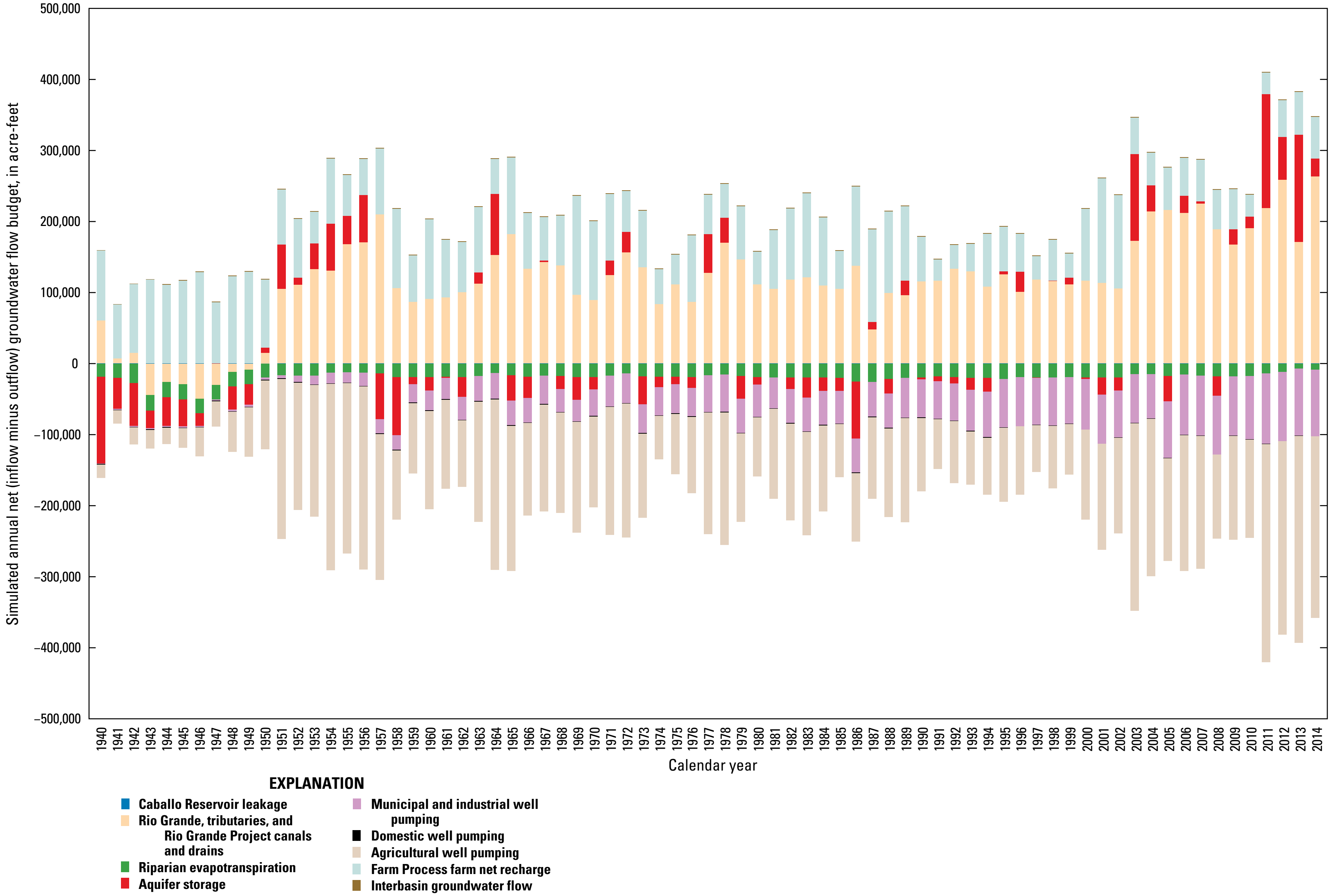

Figure 3. Simulated annual net (inflow minus outflow) groundwater flow budget by calendar year, 1940 through 2014, with budget components contributing to a net outflow from the groundwater system plotted below zero net flow and budget components contributing to a net inflow to the groundwater system plotted above zero net flow for the Rio Grande Transboundary Integrated Hydrologic Model, New Mexico and Texas, United States, and northern Chihuahua, Mexico.

For the 1950s through 2014, the surface-water system is generally losing flow to groundwater, with about a doubling of this loss from the mid-2000s onward. Most of the surface-water losses are the result of agricultural well pumping and municipal and industrial well pumping. Aquifer storage shows periods of depletion and accumulation, with most depletion (early to mid-1950s and mid-2000s to 2014) corresponding to periods of increased agricultural, municipal, and industrial well pumping.

Model Performance, Limitations, and Suggestions for Future Work

The performance and limitations of the updated and recalibrated RGTIHM are discussed in this section by evaluating mass balance errors and comparing model simulated values against measured, estimated, or reported values. The mass balance errors quantify the accuracy of the matrix solution associated with the simulation and provide context for the uncertainty of various hydrologic budget components (Reilly and Harbaugh, 2004). Measurements of head and surface-water flows were used as observations to aid in calibrating model parameters controlling hydraulic conductivity and storage properties of model layers and streambed hydraulic conductivity within the SFR2 package, among others. Estimates of agricultural pumping and reported RGP surface-water deliveries and canal waste were used as observations to aid in calibrating model parameters, such as fractional splits along the SFR2 network and OFEs, that control the dynamic simulation of these hydrologic components by the FMP. Estimates of decadal aquifer storage changes derived from groundwater level changes were used as observations to constrain the calibration of model parameters and reduce the bias to oversimulate aquifer storage depletion in the RGTIHM documented in Hanson and others (2020). Suggestions for future work with the RGTIHM are also provided.

Mass Balance

The mass balance performance of the updated and recalibrated RGTIHM was evaluated using percent and absolute volume errors for all 1,796 semimonthly time steps and annual absolute volume errors from 1940 through 2014. The percent error for each time step was calculated as

$$percent\ error = \frac{\frac{Vi - Vo}{Vi} + \frac{Vi - Vo}{Vo}}{2} \times 100\% \qquad (1)$$

where

Vi is the sum of all volumetric rate inflows to the groundwater system for each time step, and

Vo is the sum of all volumetric rate outflows from the groundwater system for each time step.

The absolute volume error for each time step was calculated as

$$absolute\ volume\ error = abs([Vi \times t] - [Vo \times t]) \qquad (2)$$

where

abs is the absolute value of the expression in parentheses, and

t is the temporal length of each time step.

The annual absolute volume error was calculated by summing all absolute volume errors for each time step in a calendar year.

The average percent error for all time steps was −0.31 percent, indicating a slight bias towards more outflows than inflows. The minimum, maximum, and standard deviation of percent errors were −4.9, 1.2, and 0.64 percent, respectively. The average absolute volume error for all time steps was 63 acre-ft, and the average annual absolute volume error was 1,500 acre-ft. The minimum, maximum, and standard deviation of annual absolute volume errors were 400; 9,700; and 2,000 acre-ft, respectively. The largest mass balance errors happened for the last 5 years of the simulation (2010 through 2014), corresponding to the largest volumes of inflows and outflows simulated by the RGTIHM (fig. 3). Overall, the mass balance errors represented a small fraction of the total inflows and outflows simulated by the RGTIHM, and the results for most hydrologic budget components were greater than the noise generated by these errors. However, hydrologic budget components with an annual absolute net value less than the average annual absolute volume error of 1,500 acre-ft ("Caballo Reservoir leakage," "domestic well pumping," and "interbasin groundwater flow" on fig. 3) were within the noise generated by the mass balance errors and could not be accurately resolved.

Hydraulic Head

The versions of the RGTIHM documented in Hanson and others (2020) and this report were calibrated to 59,130 observations of head that were spatially and temporally distributed throughout the model (see Hanson and others, 2020). The updated and recalibrated RGTIHM had an average residual (simulated minus measured head) of 10.95 ft and a median residual of 6.76 ft, and the residuals ranged from about −176.90 to 100.28 ft, with a standard deviation of 15.32 ft. The root-mean-square error (RMSE), calculated as

$$RMSE = \sqrt{\frac{\sum_{i=1}^{N}(S - M)^2}{N}} \qquad (3)$$

where

N is the total number of simulated/measured pairs,

i is the ith simulated/measured pair,

S is the simulated value associated with the ith measured value, and

M is the ith measured value,

was 18.83 ft, which represents about 2.3 percent of the 807 ft range in measured head values. About 88 percent of all simulated heads were within 30 ft of the measured values. Overall, the updated and recalibrated RGTIHM tended to oversimulate measured heads, especially at lower measured heads (fig. 4). A correlation graph of simulated against measured heads indicated a generally adequate fit across the wide range of measured heads, with some undersimulation occurring at higher measured heads (fig. 4).

There are two wells with simulated heads that do not correlate well with the measured heads (fig. 4). The poor performance of simulated heads at these two wells is most likely a result of generalizations in the spatial and vertical discretization of the model. Well RV_RC44 is located in a cell with layer 3 (upper Santa Fe Group) as the uppermost active layer, but the measured heads at the well behave in a manner similar to that of nearby wells located in model cells with layer 1 (Quaternary alluvium) as the uppermost active layer. Because the model cell in which well RV_RC44 is located is adjacent to wells with layer 1 as the uppermost active layer, it is likely that the well is located in the Quaternary alluvium and would better simulate the measured heads if it was modeled in the Quaternary alluvium. Well RV_RC112 shares its location with four other wells, all of which have simulated heads that correlate well with their measured heads. The other four wells are shallower, and their depths place them in the top two layers of the model (Quaternary alluvium). Well RV_RC112 is more than twice as deep as the other wells and is in layer 5 (middle Santa Fe Group) of the model. While the measured heads of all five of these wells are very similar, the simulated head for well RV_RC112 is considerably lower and more variable than the simulated heads of the others, suggesting that the inability of the RGTIHM to adequately simulate heads in well RV_RC112 is related to the model vertical discretization at this location.

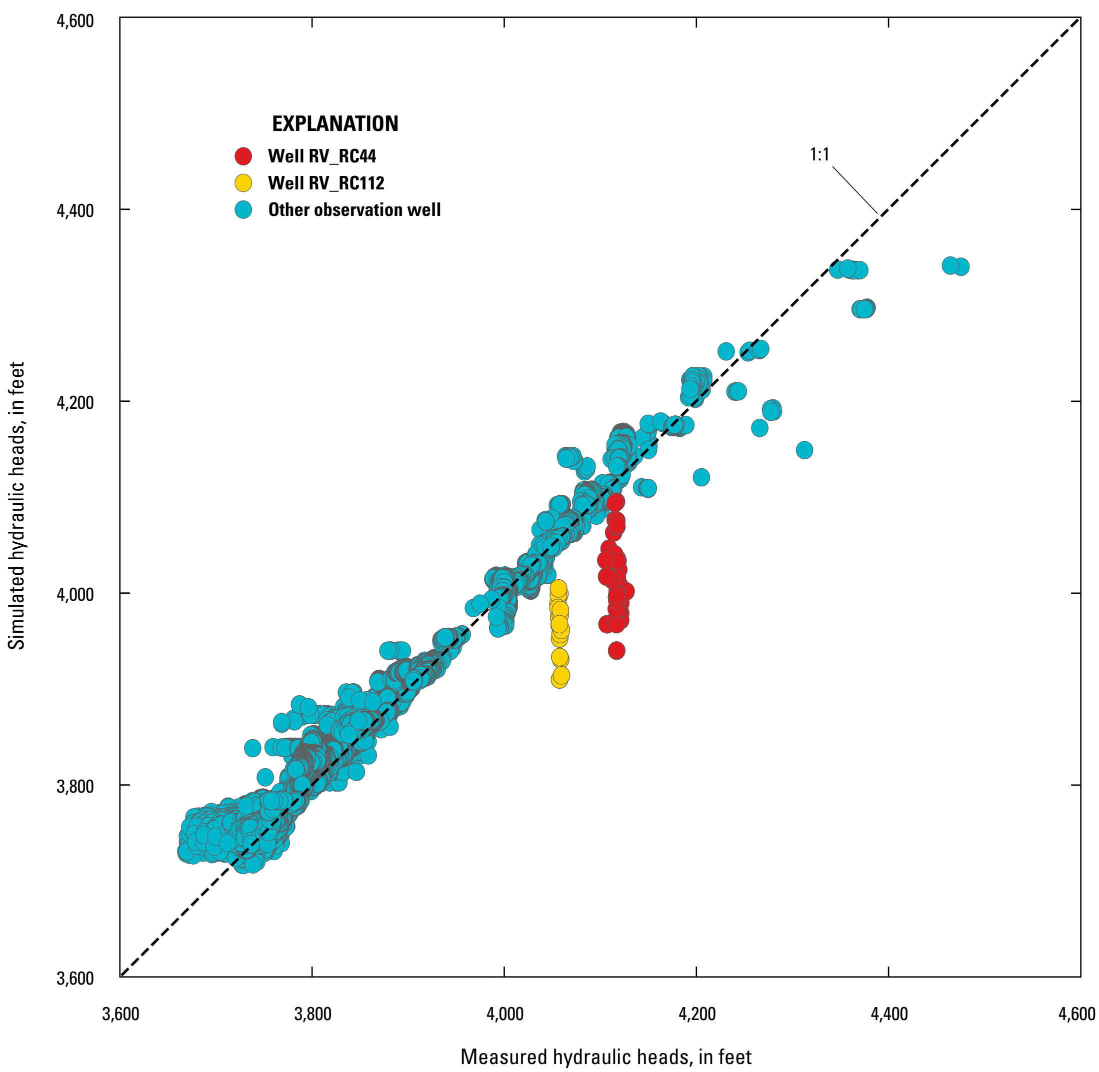

Figure 4. Correlation of simulated against measured (Ritchie and others, 2018) hydraulic heads at observation wells in the Rio Grande Transboundary Integrated Hydrologic Model, New Mexico and Texas, United States, and northern Chihuahua, Mexico.

Cumulative distribution plots of the head residuals from Hanson and others (2020) and this study indicate that there was some degradation in the simulation of heads with the update and recalibration of the RGTIHM (fig. 5). The degradation in the simulation of heads is expected because of the focus that was placed on surface-water flows and RGP surface-water deliveries and canal waste in this study (see “Model Recalibration” section). In this study, the residual distribution is oversimulated with a distribution that is approximately normal. About 76 percent of all head residuals were within one standard deviation of the average residual, about 94 percent of all head residuals were within two standard deviations of the average residual, and about 98 percent of all head residuals were within three standard deviations of the average residual.

Surface-Water Flows

As discussed in the “Model Updates” section, streamflow data from Rio Grande at El Paso were used as a key proxy for model performance relative to surface-water flows. The performance of the versions of the RGTIHM documented in Hanson and others (2020) and this report at Rio Grande at El Paso was evaluated using recommended guidance from Harmel and others (2014, 2018) and Moriasi and others (2015), which suggests using quantitative performance measures and graphical methods. The quantitative performance was evaluated using the Nash-Sutcliffe model efficiency coefficient, percent bias, and coefficient of determination (R^2). Moriasi and others (2015) provided performance evaluation criteria ranging from “not satisfactory” to “very good” for these quantitative measures for watershed-scale flow models.

The updated and recalibrated RGTIHM improves upon the simulation of monthly Rio Grande at El Paso surface-water-flow volumes as compared to the RGTIHM documented in Hanson and others (2020). The Nash-Sutcliffe model efficiency coefficient between measured and simulated Rio Grande at El Paso flows was 0.86 in Hanson and others (2020) and 0.96 in this study, both “very good” according to Moriasi and others (2015). However, the percent bias between measured and simulated Rio Grande at El Paso flows was 14 percent (“satisfactory” according to Moriasi and others [2015]) in Hanson and others (2020) and 3.5 percent (“very good” according to Moriasi and others [2015]) in this study, indicating an overall reduction in the oversimulation of measured flows in this study. The R^2 between measured and simulated Rio Grande at El Paso flows was 0.92 in Hanson and others (2020) and 0.96 in this study, both “very good” according to Moriasi and others (2015). However, the linear regression gradient (which for good agreement between measured and simulated should be close to 1) and intercept (which for good agreement between measured and simulated should be close to zero) were improved in this study (1.03 and 310 acre-ft, respectively) from Hanson and others (2020) (1.11 and 1,100 acre-ft, respectively). In addition to the quantitative measures described in Moriasi and others (2015), the cumulative residual (simulated minus measured monthly Rio Grande at El Paso surface-water-flow volumes) was computed for

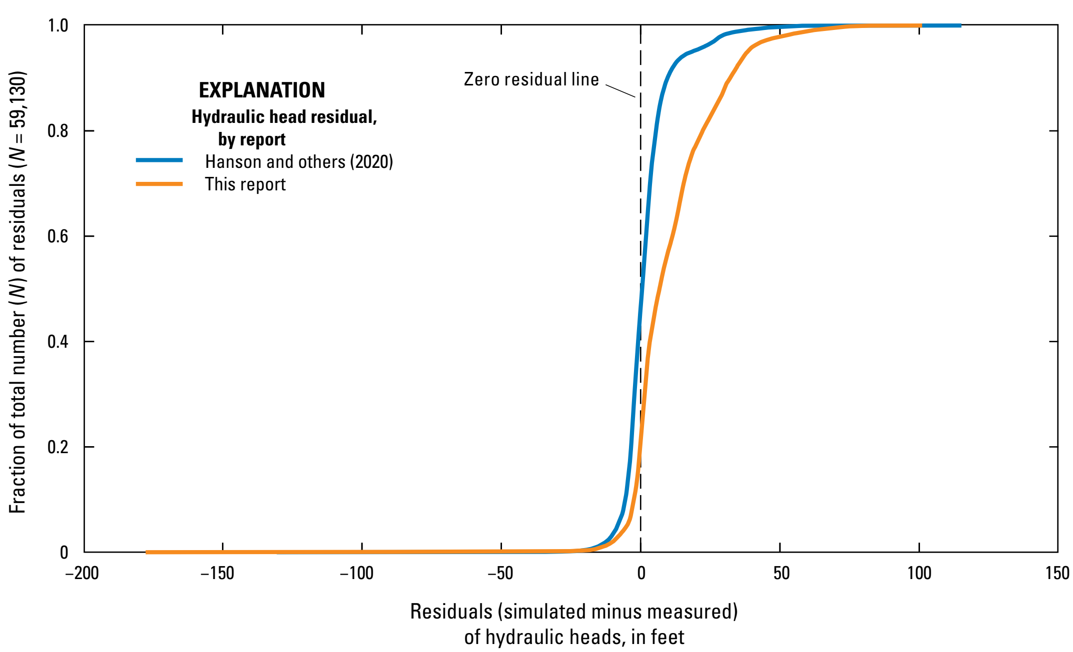

Figure 5. Cumulative distribution of hydraulic head residuals (simulated minus measured [Ritchie and others, 2018]) at observation wells in the Rio Grande Transboundary Integrated Hydrologic Model, New Mexico and Texas, United States, and northern Chihuahua, Mexico, documented in Hanson and others (2020) and this report.

the full transient simulation period (1940 through 2014). The cumulative residual at the end of the simulation period was 4.1 Macre-ft in Hanson and others (2020) and 1.0 Macre-ft in this study.

The performance of the versions of the RGTIHM documented in Hanson and others (2020) and this report was also evaluated separately for all monthly surface-water-flow measurements on the Rio Grande, RGP canals, and RGP drains that were used in the calibration of both models. The average residual (simulated minus measured monthly surface-water-flow volumes) on the Rio Grande was 7,700 acre-ft in Hanson and others (2020) and −370 acre-ft in this study, indicating an overall reduction in the oversimulation of measured Rio Grande flows in this study. The RMSE for surface-water flows on the Rio Grande was 19,000 acre-ft in Hanson and others (2020) and 8,300 acre-ft in this study. The performance of the versions of the RGTIHM relative to surface-water flows on RGP canals and drains was similar, with a slight lowering of the RMSE on RGP canals from 1,800 acre-ft in Hanson and others (2020) to 1,200 acre-ft in this study and on RGP drains from 920 acre-ft in Hanson and others (2020) to 870 acre-ft in this study.

Cumulative distribution plots of the monthly residuals on the Rio Grande, RGP canals, and RGP drains from Hanson and others (2020) and this report are shown in figure 6, illustrating the overall reduction in the oversimulation of measured Rio Grande flows in this study and the similarity in the simulation of RGP canal and drain flows in both versions of the RGTIHM. The long negative tail in the cumulative distribution plot of Rio Grande residuals in this report is the result of the undersimulation of measured Rio Grande flows at the Rio Grande below American Dam at El Paso, Tex., streamgage (Rio Grande below American Dam; USGS site number 08365000; fig. 1) from May through July 1942, when high surface-water flows were observed along the Rio Grande in the study area. The Rio Grande below American Dam streamgage is approximately 2.3 river miles downstream from the Rio Grande at El Paso streamgage and about 0.6 river miles downstream from the location where surface water is diverted for use in the El Paso Valley (fig. 1). Simulated Rio Grande at El Paso flows closely match measured flows, and simulated diversions to the El Paso Valley match measured diversions from May through July 1942, suggesting that the undersimulation of Rio Grande below American Dam flows could be the result of inflows to the Rio Grande below the dam (surface water and [or] groundwater) that are not accounted for in the RGTIHM.

Agricultural Pumping

The versions of the RGTIHM documented in Hanson and others (2020) and this report were calibrated to estimates of annual agricultural pumping obtained from various sources (see Hanson and others, 2020). These estimates indicate that annual agricultural pumping in the study area was generally less than 100,000 acre-ft from 1975 to 2000; was 100,000–150,000 acre-ft in the 2000s; and nearly doubled to 250,000–280,000 acre-ft in the early 2010s (fig. 7). It is important to note that the estimates from 1975 to 2005 and for 2010 were compiled for a different area (Doña Ana County, N. Mex.; fig. 1) than were the estimates in 2009 and from 2011 to 2014 (New Mexico Office of the State Engineer Lower Rio Grande Water Master District; fig. 1). Overall, the updated and recalibrated RGTIHM improves upon the simulation of estimated agricultural pumping as compared to Hanson and others (2020). The R^2 between estimated and simulated agricultural pumping was 0.88 in Hanson and others (2020) and 0.99 in this study. However, the linear regression gradient and intercept were degraded in this study (0.95 and 14,000 acre-ft, respectively) from Hanson and others (2020) (0.96 and 6,200 acre-ft, respectively), which manifests as a tendency to oversimulate at lower estimated agricultural pumping in this study. The RMSE was 29,000 acre-ft in Hanson and others (2020) and 12,000 acre-ft in this study. The median residual (simulated minus estimated) was 8,900 acre-ft in Hanson and others (2020) and 7,700 acre-ft in this study. The improved performance of the RGTIHM in simulating estimates of agricultural pumping adds more confidence to the simulated agricultural pumping in years without estimates (fig. 3) as compared to Hanson and others (2020).

Rio Grande Project Surface-Water Deliveries and Canal Waste

The performance of the updated and recalibrated RGTIHM relative to RGP surface-water deliveries for irrigation was evaluated by comparing annual surface-water deliveries (sum of monthly volumes in each calendar year) compiled from Reclamation's monthly water distribution reports with annual surface-water deliveries simulated by the RGTIHM from 1940 through 1978 at the valley spatial resolution (Hatch and Mesilla Valleys). As discussed in the "Model Updates" section, RGP surface-water deliveries were used as an allotment constraint on the volume of surface water that could be delivered to the WBSs simulated by the FMP in this study. Thus, in this study the surface-water deliveries simulated by the RGTIHM are never larger than the reported surface-water deliveries. However, the RGTIHM documented in Hanson and others (2020) did not use the reported surface-water deliveries as a calibration or allotment constraint and can have simulated deliveries larger than reported deliveries.

The updated and recalibrated RGTIHM improves the simulation of RGP surface-water deliveries as compared to Hanson and others (2020) (fig. 8). The R^2 between reported and simulated surface-water deliveries in the Hatch Valley and Mesilla Valley was 0.036 and 0.38 (both "not satisfactory" according to Moriasi and others [2015]), respectively, in Hanson and others (2020) and 0.97 and 0.98 (both "very good" according to Moriasi and others [2015]), respectively, in this study. The linear regression gradient and intercept in the

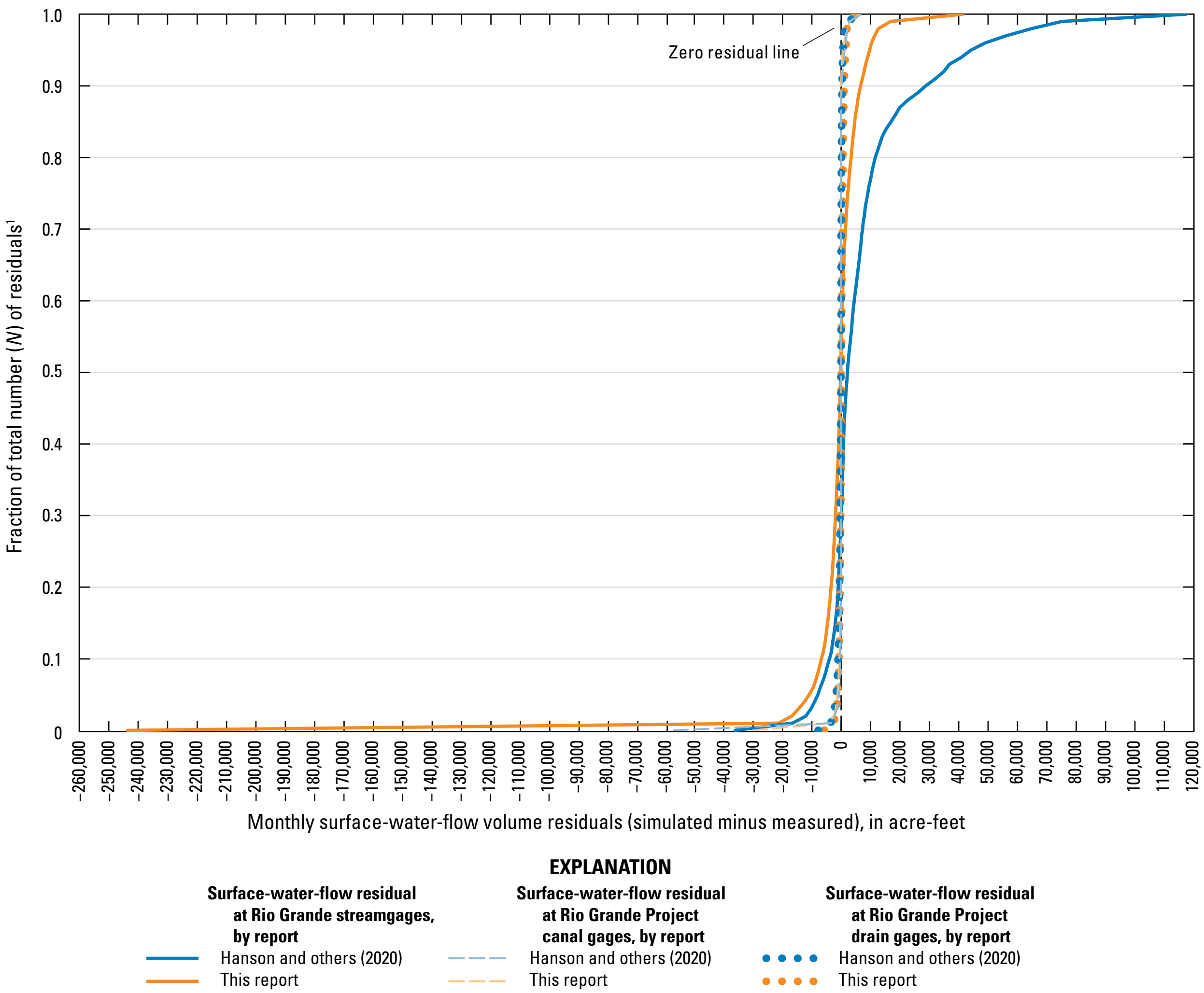

[1]*N* = 4,571 for Rio Grande streamgages; *N* = 10,301 for Rio Grande Project canal gages; and *N* = 10,845 for Rio Grande Project drain gages

Figure 6. Cumulative distribution of surface-water-flow residuals (simulated minus measured [Ritchie and others, 2018]) at Rio Grande streamgages, Rio Grande Project canal gages, and Rio Grande Project drain gages for the Rio Grande Transboundary Integrated Hydrologic Model, New Mexico and Texas, United States, and northern Chihuahua, Mexico, documented in Hanson and others (2020) and this report.

Hatch Valley (approximately 0.84 and −1,400 acre-ft, respectively) and Mesilla Valley (approximately 0.82 and −4,500 acre-ft, respectively) were improved in this study from Hanson and others (2020) in the Hatch Valley (approximately 0.067 and 17,000 acre-ft, respectively) and Mesilla Valley (approximately 0.21 and 55,000 acre-ft, respectively). The RGTIHM documented in this report shows an increasing residual (simulated minus reported) with increasing reported volume in both valleys. The larger residuals, indicating increased undersimulation of reported values, predominantly happen during the start (March and April) of the primary irrigation season in the valleys. These differences are likely the result of operational practices not captured by the FMP in the RGTIHM, such as initial wetting of agricultural fields at the start of the irrigation season that requires increased surface-water deliveries when crop transpiration is low. The low crop transpiration during this period would result in low agricultural demand and thus low surface-water deliveries simulated by the FMP in the RGTIHM. The agricultural demand (agricultural consumptive use divided by OFE) simulated by the FMP in the updated and recalibrated RGTIHM is less than the reported RGP surface-water deliveries primarily during March and April, which supports this hypothesis.

The RMSE in the Hatch Valley and Mesilla Valley was 18,000 acre-ft and 100,000 acre-ft, respectively, in Hanson and others (2020) and 7,200 acre-ft and 38,000 acre-ft, respectively, in this study. The median residual (simulated minus reported) in the Hatch Valley and Mesilla Valley was −13,000 acre-ft and −69,000 acre-ft, respectively, in Hanson and others (2020) and −6,500 acre-ft and −37,000 acre-ft, respectively, in this study. Both versions of the RGTIHM have a bias towards undersimulating reported surface-water deliveries, but the

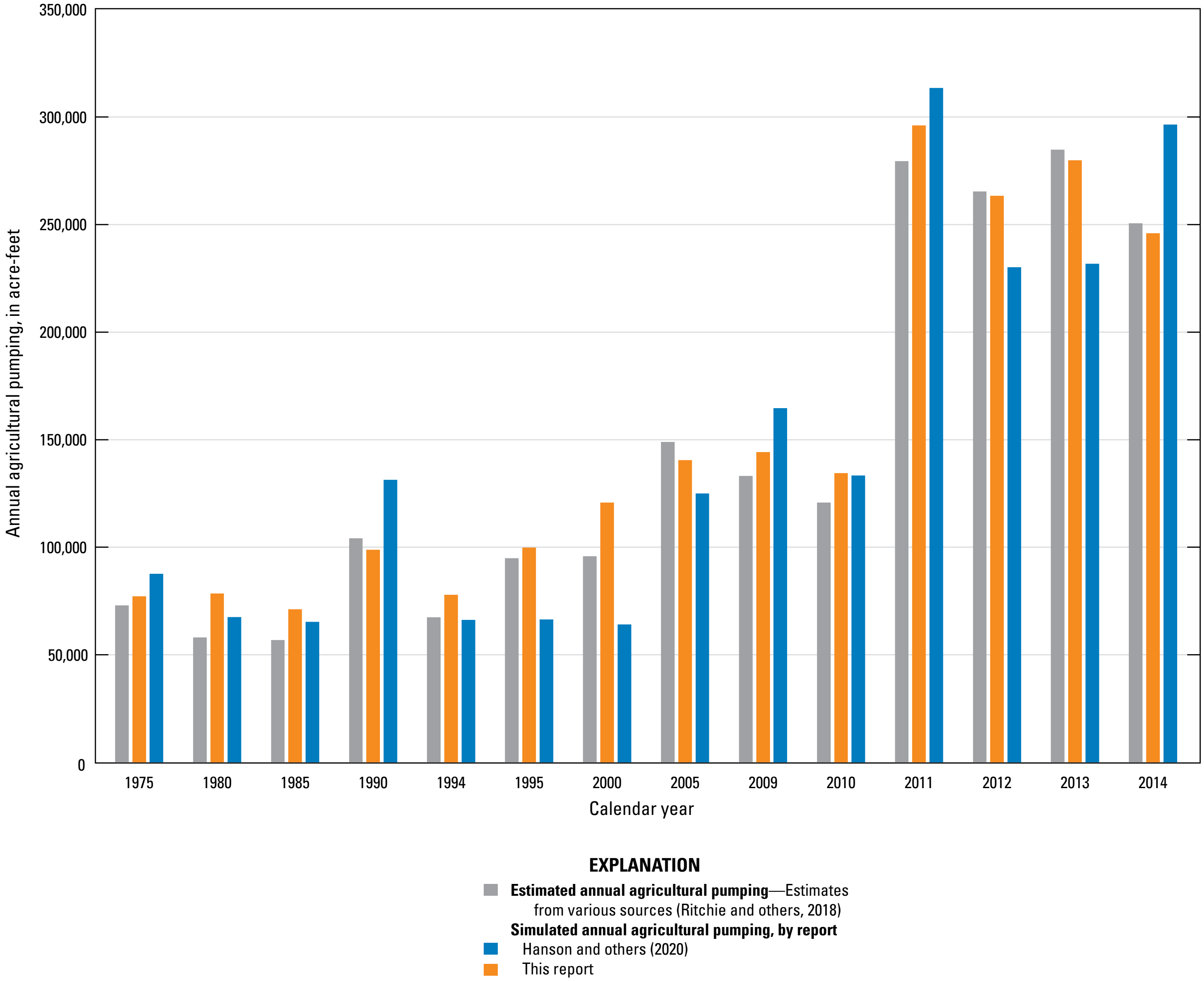

Figure 7. Comparison of estimated and simulated annual agricultural pumping for the Rio Grande Transboundary Integrated Hydrologic Model, New Mexico and Texas, United States, and northern Chihuahua, Mexico, documented in Hanson and others (2020) and this report.

version of the RGTIHM documented in this report was able to reduce that bias. The biases are larger in the Mesilla Valley, but the annual volumes of reported surface-water deliveries are also larger in the Mesilla Valley (fig. 8).

Although this study improves the simulation of RGP surface-water deliveries, the ability of the model to match reported surface-water deliveries is likely limited by the coarser spatial distribution of the reported data relative to the more refined spatial distribution of the model. As discussed in the “Model Updates” section, the surface-water delivery data disaggregated to the six agricultural service areas by Schorr and Kikuchi (2019) were further spatially disaggregated to each WBS in the RGTIHM that was supplied surface water. This spatial disaggregation was based on the fraction of the area of a WBS relative to the area of all WBSs associated with a service area. However, reported data do not exist to constrain the amount of surface water that was delivered to each WBS in the RGTIHM. Thus, the spatial disaggregation may overestimate or underestimate the surface-water deliveries to individual WBSs. An alternative spatial disaggregation approach based on the agricultural consumptive use of a WBS relative to the consumptive use of all WBSs associated with a service area was considered in this study. This alternate spatial disaggregation approach did not appear to have a major impact on model simulated deliveries.

The performance of the updated and recalibrated RGTIHM relative to RGP canal waste was evaluated by comparing annual canal waste (sum of monthly volumes in each calendar year) compiled from Reclamation’s monthly water distribution reports with annual canal waste simulated by the

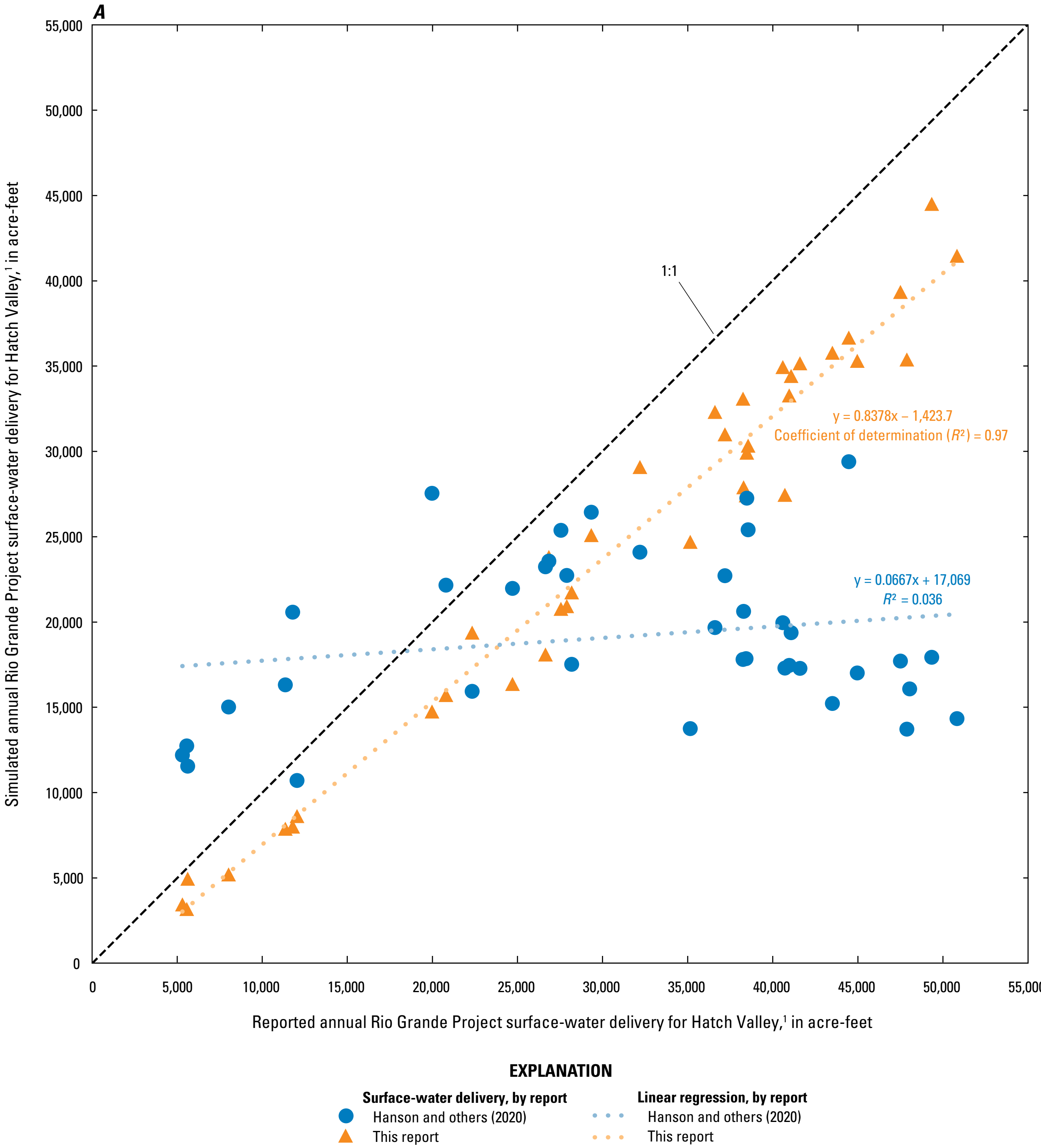

[1]Also known as Rincon Valley in the study area

Figure 8. Correlation of simulated against reported (Ritchie and others, 2022) Rio Grande Project surface-water deliveries for the *A*, Hatch Valley and *B*, Mesilla Valley for the Rio Grande Transboundary Integrated Hydrologic Model, New Mexico and Texas, United States, and northern Chihuahua, Mexico, documented in Hanson and others (2020) and this report.

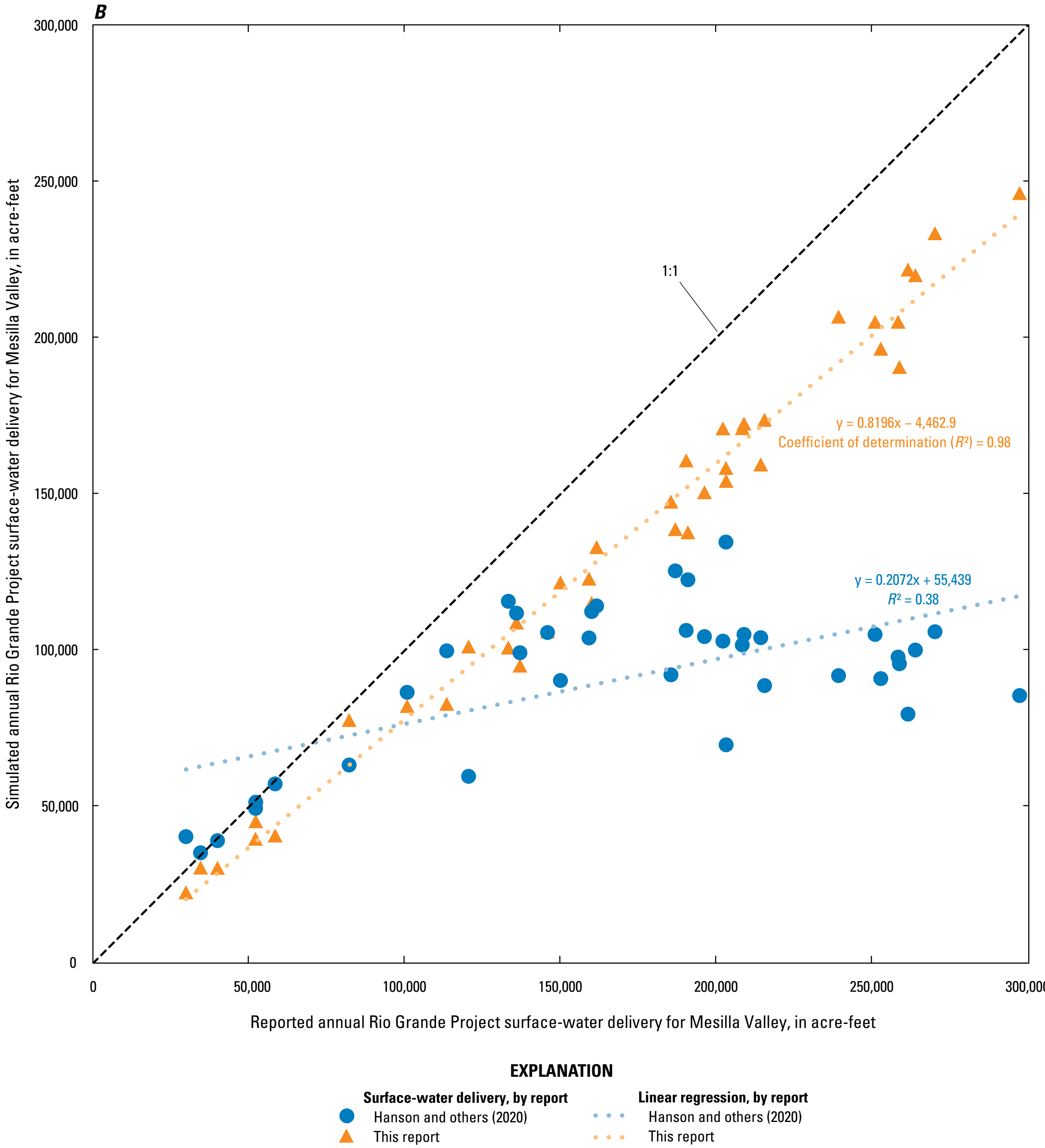

Figure 8. Correlation of simulated against reported (Ritchie and others, 2022) Rio Grande Project surface-water deliveries for the *A*, Hatch Valley and *B*, Mesilla Valley for the Rio Grande Transboundary Integrated Hydrologic Model, New Mexico and Texas, United States, and northern Chihuahua, Mexico, documented in Hanson and others (2020) and this report.—Continued

RGTIHM from 1940 through 1978 at the valley spatial resolution (Hatch and Mesilla Valleys [combination of Leasburg and Mesilla operational units]). Reported canal waste was not used as an observation dataset for calibration of the version of the RGTIHM documented in Hanson and others (2020). Thus, the version of the RGTIHM documented in this report had the benefit of including reported canal waste as an additional constraint on model calibration.

The updated and recalibrated RGTIHM improves upon the simulation of RGP canal waste as compared to Hanson and others (2020) (fig. 9). The R^2 between reported and simulated canal waste in the Hatch Valley and Mesilla Valley was 0.61 and 0.12 ("satisfactory" and "not satisfactory" according to Moriasi and others [2015]), respectively, in Hanson and others (2020) and 0.60 and 0.37 (both "not satisfactory" according to Moriasi and others [2015]), respectively, in this study. However, the linear regression gradient and intercept in the Hatch Valley (approximately 0.82 and 310 acre-ft, respectively) and Mesilla Valley (approximately 0.58 and 18,000 acre-ft, respectively) were generally improved in this study from Hanson and others (2020) in the Hatch Valley (approximately 2.9 and 2,900 acre-ft, respectively) and Mesilla Valley (approximately 1.1 and 38,000 acre-ft, respectively). The larger R^2 in the Hatch Valley in Hanson and others (2020) as compared to this study manifested as a bias to oversimulate reported canal waste in Hanson and others (2020). The RMSE in the Hatch Valley and Mesilla Valley was 30,000 acre-ft and 96,000 acre-ft, respectively, in Hanson and others (2020) and 4,100 acre-ft and 24,000 acre-ft, respectively, in this study. The median residual (simulated minus reported) in the Hatch Valley and Mesilla Valley was 22,000 acre-ft and 24,000 acre-ft, respectively, in Hanson and others (2020) and −2,000 acre-ft and −2,900 acre-ft, respectively, in this study. The median residuals highlight that Hanson and others (2020) had a bias towards oversimulating reported canal waste while this study had a bias towards undersimulating reported canal waste, although the version of the RGTIHM documented in this report was able to reduce the absolute bias. Like for RGP surface-water deliveries, the biases are larger in the Mesilla Valley, but the annual volumes of reported canal waste are also larger in the Mesilla Valley.

Decadal Aquifer Storage Changes

Decadal aquifer storage changes simulated by the updated and recalibrated RGTIHM are generally in agreement with those in Rinehart and others (2016), with depletion during the 1970s (−0.01 Macre-ft [this study] and −0.06 Macre-ft [Rinehart and others, 2016]) and 2000s (−0.10 Macre-ft [this study] and −0.05 Macre-ft [Rinehart and others, 2016]) and accumulation during the 1980s (0.16 Macre-ft [this study] and 0.14 Macre-ft [Rinehart and others, 2016]). However, the updated and recalibrated RGTIHM simulates storage accumulation during the 1960s (0.06 Macre-ft) and 1990s (0.01 Macre-ft), whereas Rinehart and others (2016) estimated depletion (−0.02 Macre-ft during the 1960s and −0.10 Macre-ft during the 1990s). Most of the storage accumulation happens in layer 1 of the model and is derived from deep percolation to groundwater from the WBSs and surface-water losses. Attempts to improve the RGTIHM's simulation of aquifer storage changes relative to Rinehart and others (2016) resulted in the degradation of the simulation of measured surface-water flows, particularly at Rio Grande at El Paso. The RGTIHM documented in Hanson and others (2020) generally simulated greater storage depletion than estimated by Rinehart and others (2016) and simulated in this study, with depletion of −0.17, −0.34, −0.09, and −0.72 Macre-ft during the 1960s, 1970s, 1990s, and 2000s, respectively.

Limitations and Suggestions for Future Work

Although the updated and recalibrated RGTIHM documented in this report was able to improve the simulation of measured surface-water flows and reported RGP surface-water deliveries and canal waste relative to Hanson and others (2020), there was a degradation in the simulation of measured heads in this study relative to Hanson and others (2020). Despite this degradation, the simulation of measured heads in the updated and recalibrated RGTIHM remains robust. However, future work with the RGTIHM that involves extending the simulation period should incorporate new (post-2014) measurements of head to verify model performance. The agricultural pumping estimates used for recalibration in this study were compiled annually for all wells in large regions (Doña Ana County and New Mexico Office of the State Engineer Lower Rio Grande Water Master District). Future work with the RGTIHM that involves extending the simulation period should consider incorporating more temporally (monthly or seasonally) and spatially (individual or groups of wells) refined estimates of agricultural pumping to verify model performance.

The spatial resolution of agricultural land use in the RGTIHM (WBSs) was finer than the spatial resolution of the data used to estimate agricultural consumptive use and surface-water deliveries to these WBSs. Thus, the methods used to spatially disaggregate agricultural consumptive use and surface-water deliveries to each WBS are uncertain and may result in the overestimation or underestimation of these components within individual WBSs. More spatially refined estimates of agricultural consumptive use would likely improve the simulation capability of the RGTIHM and may be considered for future work. An alternative approach to spatially disaggregate reported surface-water deliveries based on the agricultural consumptive use of a WBS relative to the consumptive use of all WBSs associated with a service area may benefit from more spatially refined estimates of consumptive use and may be considered for future work with the RGTIHM. RGP surface-water deliveries to each WBS were used as an allotment constraint in this study, but because of the uncertainty associated with the spatial disaggregation of

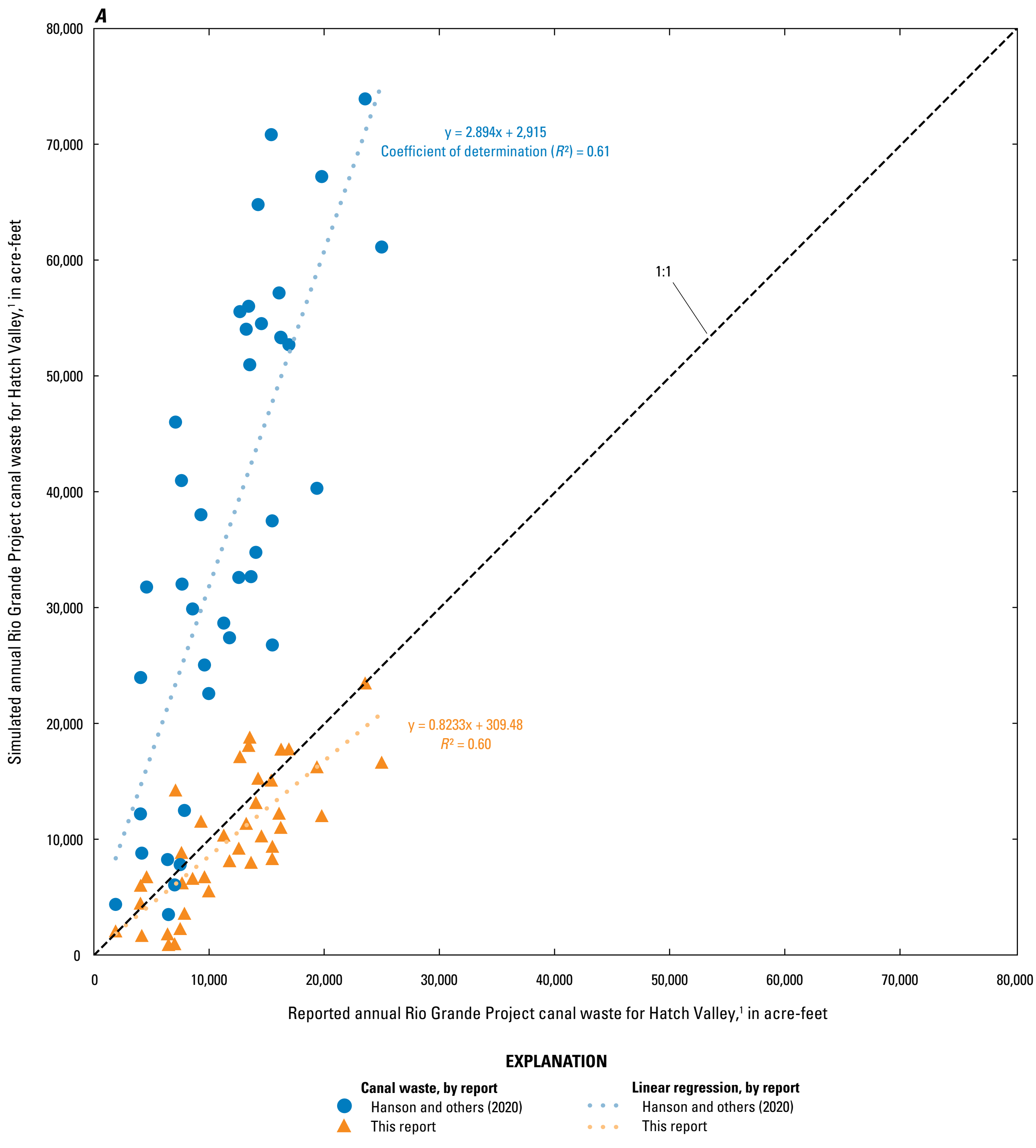

[1]Also known as Rincon Valley in the study area

Figure 9. Correlation of simulated against reported (Ritchie and others, 2022) Rio Grande Project canal waste for the *A*, Hatch Valley and *B*, Mesilla Valley for the Rio Grande Transboundary Integrated Hydrologic Model, New Mexico and Texas, United States, and northern Chihuahua, Mexico, documented in Hanson and others (2020) and this report.

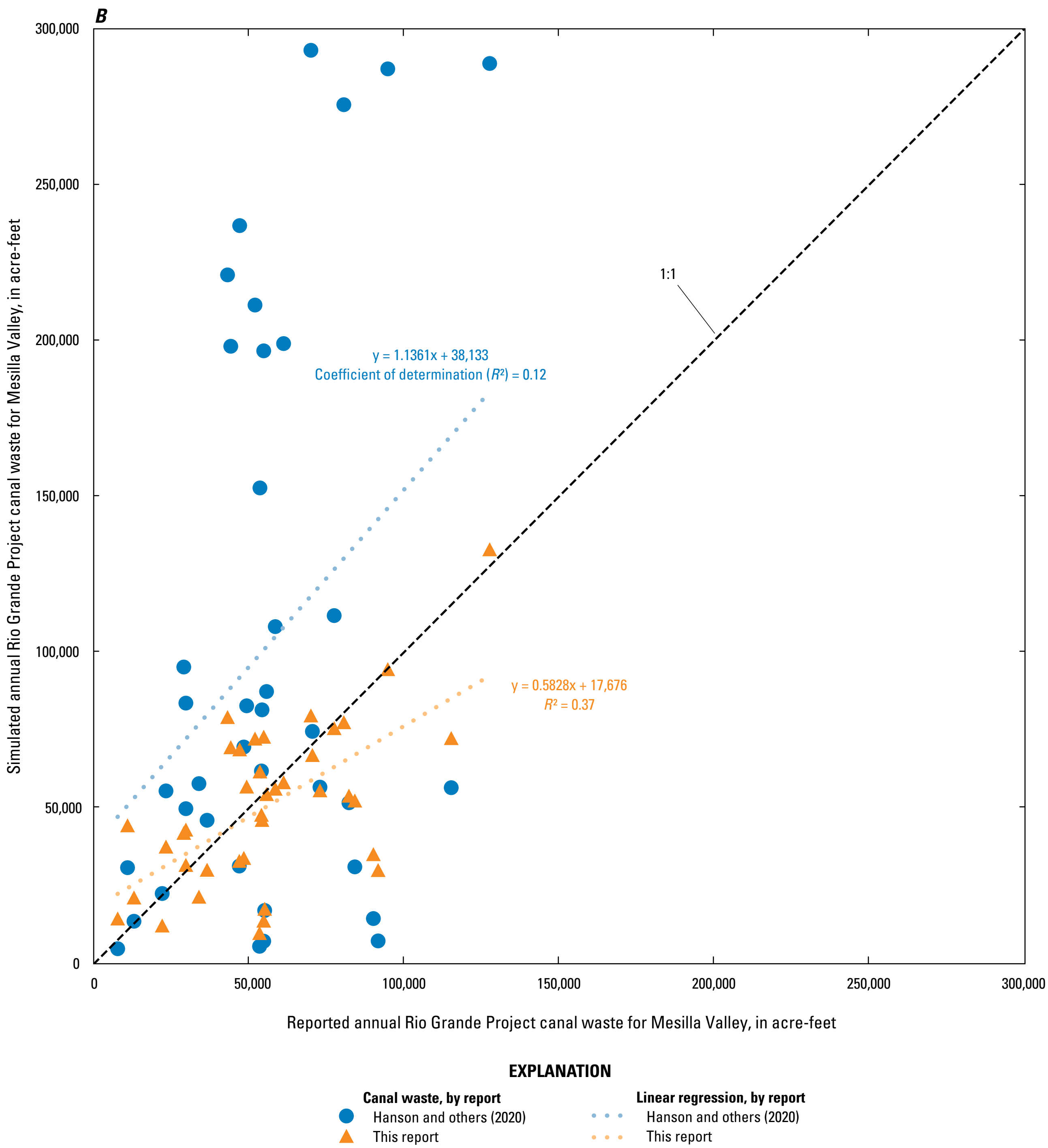

Figure 9. Correlation of simulated against reported (Ritchie and others, 2022) Rio Grande Project canal waste for the *A*, Hatch Valley and *B*, Mesilla Valley for the Rio Grande Transboundary Integrated Hydrologic Model, New Mexico and Texas, United States, and northern Chihuahua, Mexico, documented in Hanson and others (2020) and this report.—Continued

these deliveries to individual WBSs, future efforts with the RGTIHM may consider removing or relaxing this constraint to prevent biases in the simulation. Future work is also merited in order to investigate the annual variability of OFEs, their correlation with irrigation supply and demand, and potential parameter compensation.

The RGTIHM's simulation of aquifer storage change is likely limited by a variety of factors, including the spatial and temporal resolution of the model and the parameterization of storage properties for model layers simulated as confined that are unconfined. As discussed in the "Hydraulic Conductivity and Storage Properties" section, model layers that behave in an unconfined manner are assigned a specific storage estimated as specific yield divided by the cell thickness plus the compressibility of water. The spatially variable cell thickness of layers 3 through 9 imparts a spatial variability to these "unconfined" specific storage values that is not physically based on changing lithofacies. The simulation of aquifer storage in the RGTIHM could benefit from simulating unconfined layers as convertible, allowing the model to shift between specific storage and specific yield on the basis of the head in the layer. Attempts were made to incorporate convertible layers in the update documented in this study, but convertible layers added excessive numerical instability and run times to the model that made recalibration and full transient simulations impractical.

Summary

The Rio Grande Transboundary Integrated Hydrologic Model (RGTIHM) was developed through an interagency effort between the U.S. Geological Survey and the Bureau of Reclamation to provide a tool for analyzing the hydrologic system response to the historical evolution of water use and potential changes in water supplies and demands in the Hatch Valley (also known as Rincon Valley in the study area) and Mesilla Basin, New Mexico and Texas, United States, and northern Chihuahua, Mexico. Reclamation operates the Rio Grande Project (RGP) to store and deliver surface water for irrigation and municipal use within the study area and in the El Paso Valley south of the El Paso Narrows. The RGTIHM, using version 2 of the MODFLOW One-Water Hydrologic Flow Model, provides a tool to evaluate alternative management strategies, including conjunctive management of surface water and groundwater, to support long-term planning and decision making for the RGP.

Biases in the RGTIHM's simulation of streamflow and aquifer storage depletion and the availability of new estimates of historical agricultural consumptive use in the study area initiated an update and recalibration of the RGTIHM. In addition to the new estimates of historical agricultural consumptive use, updates were made to more accurately represent the natural system and included adjustments to the initial groundwater levels; streamflow rating tables; Rio Grande, canal, and drain streambed elevations; tributary streambed elevations; surface-water inflows and diversions; RGP surface-water deliveries and canal waste; on-farm efficiency; the routing of surface-water runoff within the MODFLOW Farm Process; and general head boundaries used to simulate interbasin groundwater flow. Model settings, including the assignment of hydraulic conductivity and storage properties to model layers and the MODFLOW solver package, were adjusted to improve numerical stability, and the model was recalibrated to better simulate the natural system. Recalibration of the RGTIHM was performed using PEST, specifically BeoPEST, on the U.S. Geological Survey Denali supercomputer. Parameters that were adjusted during recalibration included horizontal hydraulic conductivity, vertical anisotropy, and specific storage of model layers; hydraulic conductance within the General-Head Boundary package; hydraulic characteristic within the Horizontal Flow Barrier package; streambed hydraulic conductivity within the Streamflow-Routing package; fractional splits of the flow in the segment upstream from diversion points along the Streamflow-Routing network where water is diverted within canal from main canals to smaller canals; and annual on-farm efficiencies for the Hatch and Mesilla Valleys.

The performance of the updated and recalibrated RGTIHM was evaluated by comparing model simulated values against measured, estimated, or reported values for hydraulic head, surface-water flows, agricultural pumping, RGP surface-water deliveries and canal waste, and decadal aquifer storage changes. Streamflow data at the Rio Grande at El Paso, Tex., streamgage (Rio Grande at El Paso; U.S. Geological Survey site number 08364000) were used as a key proxy for model performance relative to surface-water flows because the site is near the end of the surface-water network, near the terminus of the Mesilla Basin, and has a long historical measurement record spanning the full transient simulation (1940 through 2014). The updated and recalibrated RGTIHM reduced the cumulative residual (simulated minus measured) at the end of the simulation period in monthly Rio Grande at El Paso surface-water-flow volumes from 4.1 million acre-feet (Macre-ft) in the previous version of the model to 1.0 Macre-ft in this study. The updated and recalibrated RGTIHM was also able to reduce the large aquifer storage depletion simulated in the previous version of the model (−0.17, −0.34, −0.09, and −0.72 Macre-ft during the 1960s, 1970s, 1990s, and 2000s, respectively), bringing simulated decadal aquifer storage changes (0.06, −0.01, 0.16, 0.01, and −0.10 Macre-ft during the 1960s, 1970s, 1980s, 1990s, and 2000s, respectively) closer to estimates derived from groundwater level changes in an observation dataset (−0.02, −0.06, 0.14, −0.10, and −0.05 Macre-ft during the 1960s, 1970s, 1980s, 1990s, and 2000s, respectively). Model performance was also evaluated in terms of mass balance errors and conceptual understanding of the hydrologic system. Overall, the updated and recalibrated RGTIHM demonstrates a robust ability to simulate the spatially and temporally variable measurements, estimates, or reports of the hydrologic system state, with low mass balance errors and with improvements over the previous version of the model.

Acknowledgments

The authors would like to thank U.S. Geological Survey colleagues Randall Hanson (retired) and Scott Boyce for their mentorship and guidance in all things MODFLOW. Thanks also to U.S. Geological Survey colleagues Chris Langevin and Joe Hughes for their help debugging model performance issues.

References Cited

Ahadi, R., Samani, Z., and Skaggs, R., 2013, Evaluating on-farm irrigation efficiency across the watershed—A case study of New Mexico's Lower Rio Grande Basin: Agricultural Water Management, v. 124, p. 52–57.

Anderson, M.P., Woessner, W.W., and Hunt, R.J., 2015, Applied groundwater modeling—Simulation of flow and advective transport (2d ed.): San Diego, Calif., Academic Press, 564 p.

Boyce, S.E., Hanson, R.T., Ferguson, I., Schmid, W., Henson, W., Reimann, T., Mehl, S.M., and Earll, M.M., 2020, One-Water Hydrologic Flow Model—A MODFLOW based conjunctive-use simulation software: U.S. Geological Survey Techniques and Methods, book 6, chap. A60, 435 p., accessed February 24, 2022, at https://doi.org/10.3133/tm6A60.

Bureau of Reclamation, 2013, Implementation of Rio Grande Project operating procedures, New Mexico and Texas—Supplemental environmental assessment: Bureau of Reclamation, 89 p., accessed August 23, 2021, at https://www.usbr.gov/uc/albuq/envdocs/ea/riogrande/op-Proced/Supplemental/Final-SuppEA.pdf.

Doherty, J., 2019, PEST, Model-independent parameter estimation—User manual part I: PEST, SENSAN and Global Optimisers (7th ed., with additions): Brisbane, Australia, Watermark Numerical Computing.

Driscoll, J.M., and Sherson, L.R., 2016, Variability of surface-water quantity and quality and shallow groundwater levels and quality within the Rio Grande Project area, New Mexico and Texas, 2009–13: U.S. Geological Survey Scientific Investigations Report 2016–5006, 33 p., accessed March 16, 2022, at https://doi.org/10.3133/sir20165006.

Esri, 2020, World Terrain Base: Esri tile layer, accessed August 11, 2021, at https://server.arcgisonline.com/ArcGIS/rest/services/World_Terrain_Base/MapServer.

Faunt, C.C., ed., 2009, Groundwater availability of the Central Valley aquifer, California: U.S. Geological Survey Professional Paper 1766, 225 p.

Flint, L.E., Flint, A.L., and Stern, M.A., 2021, The basin characterization model—A regional water balance software package: U.S. Geological Survey Techniques and Methods 6–H1, 85 p., accessed February 24, 2022, at https://doi.org/10.3133/tm6H1.

Hanson, R.T., and Leake, S.A., 1999, Documentation for HYDMOD, a program for extracting and processing time-series data from the U.S. Geological Survey's modular three-dimensional finite-difference ground-water flow model: U.S. Geological Survey Open-File Report 98–564, 57 p.

Hanson, R.T., Ritchie, A.B., Boyce, S.E., Galanter, A.E., Ferguson, I.A., Flint, L.E., Flint, A., and Henson, W.R., 2020, Rio Grande Transboundary Integrated Hydrologic Model and water-availability analysis, New Mexico and Texas, United States, and northern Chihuahua, Mexico: U.S. Geological Survey Scientific Investigations Report 2019–5120, 186 p., accessed February 24, 2022, at https://doi.org/10.3133/sir20195120.

Harbaugh, A.W., Banta, E.R., Hill, M.C., and McDonald, M.G., 2000, MODFLOW-2000, the U.S. Geological Survey modular ground-water model—User guide to modularization concepts and the Ground-Water Flow Process: U.S. Geological Survey Open-File Report 00–92, 121 p.

Harmel, R.D., Baffaut, C., and Douglas-Mankin, K., 2018, Review and development of ASABE Engineering Practice 621—Guidelines for calibrating, validating, and evaluating hydrologic and water quality models: Transactions of the ASABE, v. 61, no. 4, p. 1393–1401, accessed February 10, 2020, at https://doi.org/10.13031/trans.12806.

Harmel, R.D., Smith, P.K., Migliaccio, K.W., Chaubey, I., Douglas-Mankin, K.R., Benham, B., Shukla, S., Muñoz-Carpena, R., and Robson, B.J., 2014, Evaluating, interpreting, and communicating performance of hydrologic/water quality models considering intended use—A review and recommendations: Environmental Modelling & Software, v. 57, p. 40–51, accessed February 10, 2020, at https://doi.org/10.1016/j.envsoft.2014.02.013.

Hawley, J.W., and Kennedy, J.F., 2004, Creation of a digital hydrogeologic framework model of the Mesilla Basin and southern Jornada del Muerto Basin: Las Cruces, N. Mex., New Mexico Water Resources Research Institute, Technical Completion Report 332, 105 p., accessed August 23, 2021, at https://nmwrri.nmsu.edu/wp-content/uploads/TR/tr332.pdf.

Hawley, J.W., and Lozinsky, R.P., 1992, Hydrogeologic framework of the Mesilla Basin in New Mexico and western Texas: New Mexico Bureau of Mines and Mineral Resources, Open-File Report 323, 55 p., accessed March 3, 2022, at https://geoinfo.nmt.edu/publications/openfile/downloads/300-399/323/ofr_323.pdf.

Hill, M.C., Banta, E.R., Harbaugh, A.W., and Anderman, E.R., 2000, MODFLOW-2000, the U.S. Geological Survey modular ground-water model—User guide to the Observation, Sensitivity, and Parameter-Estimation Processes and three post-processing programs: U.S. Geological Survey Open-File Report 00–184, 210 p.

Hsieh, P.A., and Freckleton, J.R., 1993, Documentation of a computer program to simulate horizontal-flow barriers using the U.S. Geological Survey modular three-dimensional finite difference ground-water flow model: U.S. Geological Survey Open-File Report 92–477, 32 p.

Hutchison, W.R., 2019, Expert report of William R. Hutchison in the matter of no. 141, original, in the Supreme Court of the United States, State of Texas v. State of New Mexico and State of Colorado: Sacramento, Calif., Somach Simmons & Dunn, prepared by William R. Hutchison, Jamaica Beach, Tex., 77 p.

International Boundary and Water Commission, 2015, 1-meter resolution bare-earth lidar grids delivered through ftp, referenced in Tetra Tech/Watershed Sciences, Inc. Team, 2011: International Boundary and Water Commission lidar data report, 77 p.

Jensen, M.E., 1967, Evaluation irrigation efficiency: Journal of the Irrigation and Drainage Division, American Society of Civil Engineers, v. 93, no. 1, p. 83–98.

Longworth, J.W., Valdez, J.M., Magnuson, M.L., Albury, E.S., and Keller, J., 2008, New Mexico water use by categories 2005: New Mexico State Engineer Office, Technical Report 52, 122 p.

Macfarlane, P.A., 1995, The effect of river valleys and the upper Cretaceous aquitard on regional flow in the Dakota aquifer in the central Great Plains of Kansas and southeastern Colorado: Current Research on Kansas Geology, Kansas Geological Survey, Bulletin 238, 20 p.

Magnuson, M.L., Valdez, J.M., Lawler, C.R., Nelson, M., and Petronis, L., 2019, New Mexico water use by categories 2015: New Mexico State Engineer Office, Technical Report 55.

Moriasi, D.N., Gitau, M.W., Pai, N., and Daggupati, P., 2015, Hydrologic and water quality models—Performance measures and evaluation criteria: Transactions of the ASABE, v. 58, no. 6, p. 1763–1785.

Naff, R.L., and Banta, E.R., 2008, The U.S. Geological Survey modular ground-water model—PCGN: A preconditioned conjugate gradient solver with improved nonlinear control: U.S. Geological Survey Open-File Report 2008–1331, 35 p.

Niswonger, R.G., Panday, S., and Ibaraki, M., 2011, MODFLOW-NWT, a Newton formulation for MODFLOW-2005: U.S. Geological Survey Techniques and Methods, book 6, chap. A37, 44 p., accessed June 17, 2022, at https://doi.org/10.3133/tm6A37.

Niswonger, R.G., and Prudic, D.E., 2005, Documentation of the Streamflow-Routing (SFR2) Package to include unsaturated flow beneath streams—A modification to SFR1: U.S. Geological Survey Techniques and Methods, book 6, chap. A13, 47 p.

Reilly, T.E., and Harbaugh, A.W., 2004, Guidelines for evaluating ground-water flow models: U.S. Geological Survey Scientific Investigations Report 2004–5038, 30 p.

Rinehart, A., Mamer, E., Felix, B., Kludt, T., Pokorny, C., and Timmons, S., 2016, Groundwater storage change estimates in alluvial aquifers in central New Mexico: New Mexico Bureau of Geology and Mineral Resources Technical Fact Sheet, accessed August 10, 2021, at https://geoinfo.nmt.edu/geoscience/research/documents/19/GLSC_factsheet_2016.pdf.

Ritchie, A.B., Galanter, A.E., Flickinger, A.K., Shephard, Z.M., and Ferguson, I.M., 2022, MODFLOW One-Water Hydrologic Flow Model (MF-OWHM) used to simulate conjunctive use in the Hatch Valley and Mesilla Basin, New Mexico and Texas, United States, and northern Chihuahua, Mexico: U.S. Geological Survey data release, https://doi.org/10.5066/P99PLDXV.

Ritchie, A.B., Hanson, R.T., Galanter, A.E., Boyce, S.E., Damar, N.A., Shephard, Z.M., and Tillman, F.D., 2018, Digital hydrologic and geospatial data for the Rio Grande Transboundary Integrated Hydrologic Model and water-availability analysis, New Mexico and Texas, United States, and northern Chihuahua, Mexico: U.S. Geological Survey data release, accessed February 24, 2022, at https://doi.org/10.5066/P9J9NYND.

Schmid, W., and Hanson, R.T., 2009, The Farm Process Version 2 (FMP2) for MODFLOW-2005—Modifications and upgrades to FMP1: U.S. Geological Survey Techniques and Methods, book 6, chap. A32, 102 p.

Schorr, S.W., and Kikuchi, C.P., 2019, Water budget estimates in support of groundwater model development—Rincon and Mesilla Basins, New Mexico, Texas, and northern Mexico, 1938 through 2016: Tucson, Ariz., Montgomery & Associates expert report, 207 p.

Schreüder, W.A., 2021, Running BeoPEST: Principia Mathematica, Inc., accessed February 26, 2021, at https://www.prinmath.com/pest/RunBeoPEST.pdf.

Serrano, R.J., 2015, Lower Rio Grande Water Master annual report 2014 accounting year: Las Cruces, N. Mex., State of New Mexico Office of the State Engineer, 25 p., accessed March 1, 2022, at https://www.ose.state.nm.us/WM/LRG/Reports/2014%20LRG%20Water%20Master%20Report.pdf.

S.S. Papadopulos and Associates, Inc., 2007, Draft—Groundwater flow model for administration and management in the Lower Rio Grande Basin: Boulder, Colorado, S.S. Papadopulos and Associates, Inc., draft report prepared for the New Mexico Office of the State Engineer, 380 p.

Sweetkind, D.S., 2017, Three-dimensional hydrogeologic framework model of the Rio Grande transboundary region of New Mexico and Texas, USA, and northern Chihuahua, Mexico: U.S. Geological Survey Scientific Investigations Report 2017–5060, 49 p., accessed February 24, 2022, at https://doi.org/10.3133/sir20175060.

Sweetkind, D.S., Hanson, R.T., Ritchie, A.B., and Hawley, J.W., 2017, Data release of three-dimensional hydrogeologic framework model of the Rio Grande transboundary region of New Mexico and Texas, USA and northern Chihuahua, Mexico: U.S. Geological Survey data release, accessed February 24, 2022, at https://doi.org/10.5066/F7JM27T6.

Tetra Tech EM, Inc., 2004, Report of surveying activities conducted within the Rincon and Mesilla Valleys, New Mexico—Prepared for New Mexico Interstate Stream Commission: Albuquerque, N. Mex., Tetra Tech EM, Inc., 233 p.

U.S. Geological Survey, 2013a, U.S. Geological Survey National Elevation Dataset n32w107 1/3 arc-second 2013 1 x 1 degree ArcGrid: U.S. Geological Survey National Elevation Dataset, accessed November 23, 2015, at http://ned.usgs.gov.

U.S. Geological Survey, 2013b, U.S. Geological Survey National Elevation Dataset n32w108 1/3 arc-second 2013 1 x 1 degree ArcGrid: U.S. Geological Survey National Elevation Dataset, accessed November 23, 2015, at http://ned.usgs.gov.

U.S. Geological Survey, 2013c, U.S. Geological Survey National Elevation Dataset n33w107 1/3 arc-second 2013 1 x 1 degree ArcGrid: U.S. Geological Survey National Elevation Dataset, accessed November 23, 2015, at http://ned.usgs.gov.

U.S. Geological Survey, 2013d, U.S. Geological Survey National Elevation Dataset n33w108 1/3 arc-second 2013 1 x 1 degree ArcGrid: U.S. Geological Survey National Elevation Dataset, accessed November 23, 2015, at http://ned.usgs.gov.

U.S. Geological Survey, 2013e, U.S. Geological Survey National Elevation Dataset n34w107 1/3 arc-second 2013 1 x 1 degree ArcGrid: U.S. Geological Survey National Elevation Dataset, accessed November 23, 2015, at http://ned.usgs.gov.

U.S. Geological Survey, 2013f, U.S. Geological Survey National Elevation Dataset n34w108 1/3 arc-second 2013 1 x 1 degree ArcGrid: U.S. Geological Survey National Elevation Dataset, accessed November 23, 2015, at http://ned.usgs.gov.

U.S. Geological Survey, 2016, U.S. Geological Survey National Elevation Dataset original product resolution TX RioGrand-FTWhit 2014 ArcGrid 2016 [20160628]: U.S. Geological Survey National Elevation Dataset raster digital data, accessed August 22, 2018, at http://ned.usgs.gov/.

U.S. Geological Survey Advanced Research Computing, 2021, USGS Denali supercomputer: U.S. Geological Survey website, accessed February 24, 2022, at https://doi.org/10.5066/P9PSW367.

Wilson, B.C., 1992, Water use by categories in New Mexico counties and river basins and irrigated acreage in 1990: New Mexico State Engineer Office, Technical Report 47, 141 p.

Wilson, B.C., and Lucero, A.A., 1997, Water use by categories in New Mexico counties and river basins and irrigated acreage in 1995: New Mexico State Engineer Office, Technical Report 49, 149 p.

Wilson, B.C., Lucero, A.A., Romero, J.T., and Romero, P.J., 2003, Water use by categories in New Mexico counties and river basins and irrigated acreage in 2000: New Mexico State Engineer Office, Technical Report 51, 164 p.

Wilson, C.A., White, R.R., Orr, B.R., and Roybal, R.G., 1981, Water resources of the Rincon and Mesilla Valleys and adjacent areas, New Mexico: U.S. Geological Survey Technical Report 43, 514 p.

Witcher, J.C., King, J.P., Hawley, J.W., Kennedy, J.F., Williams, J., Cleary, M., and Bothern, L.R., 2004, Sources of salinity in the Rio Grande and Mesilla Basin groundwater: New Mexico Water Resources Research Institute Technical Report no. 330, 168 p.

For more information about this publication, contact
Director, New Mexico Water Science Center
U.S. Geological Survey
6700 Edith Blvd. NE
Albuquerque, NM 87113

For additional information, visit
https://www.usgs.gov/centers/nm-water

Publishing support provided by
Lafayette Publishing Service Center

Ritchie and others—**Update and Recalibration of the Rio Grande Transboundary Integrated Hydrologic Model**—SIR 2022–5045

ISSN 2328-0328 (online)
https://doi.org/10.3133/sir20225045